



SERVIÇO PÚBLICO FEDERAL
MINISTÉRIO DA EDUCAÇÃO
UNIVERSIDADE FEDERAL DE UBERLÂNDIA
FACULDADE DE ODONTOLOGIA
PROGRAMA DE PÓS-GRADUAÇÃO

MARINA DE MELO NAVES

Características micro e macrogeométricas de implantes dentais e sua deformação no processo de instalação cirúrgica

Tese apresentada à Faculdade de Odontologia da Universidade de Uberlândia, para obtenção do Título de Doutora em Odontologia na Área de Clínica Odontológica Integrada.

Uberlândia 2015

MARINA DE MELO NAVES

**Características micro e macrogeométricas de implantes dentais
e sua deformação no processo de instalação cirúrgica**

Tese apresentada à Faculdade de Odontologia da Universidade de Uberlândia, para obtenção do Título de Doutora em Odontologia na Área de Clínica Odontológica Integrada.

Orientador: Prof. Dr. Denildo de Magalhães
Co-Orientadora: Prof^a. Dra. Henara Lillian Costa

Banca examinadora:
Prof. Dr. César Bataglion
Prof. Dr. Wilson Matsumoto
Prof. Dr. Denildo de Magalhães
Prof. Dr. Paulo César Simamoto Júnior
Prof. Dr. Luis Henrique Araújo Raposo

Uberlândia 2015

Dados Internacionais de Catalogação na Publicação (CIP)
Sistema de Bibliotecas da UFU, MG, Brasil.

N323c
2015

Naves, Marina de Melo, 1985-
Características micro e macrogeométricas de implantes dentais e sua
deformação no processo de instalação cirúrgica / Marina de Melo Naves.
- 2015.
63 f. : il.

Orientador: Denildo de Magalhães.
Coorientadora: Henara Lilian Costa.
Tese (doutorado) - Universidade Federal de Uberlândia, Programa
de Pós-Graduação em Odontologia.
Inclui bibliografia.

1. Odontologia - Teses. 2. Implantes dentários - Teses. I. Magalhães,
Denildo de. II. Costa, Henara Lilian. III. Universidade Federal de
Uberlândia. Programa de Pós-Graduação em Odontologia. IV. Título.

CDU: 616.314



SERVIÇO PÚBLICO FEDERAL
MINISTÉRIO DA EDUCAÇÃO
UNIVERSIDADE FEDERAL DE UBERLÂNDIA
FACULDADE DE ODONTOLOGIA



PROGRAMA DE PÓS-GRADUAÇÃO EM ODONTOLOGIA

Ata da defesa de TESE DE DOUTORADO junto ao Programa de Pós-graduação em Odontologia Faculdade de Odontologia da Universidade Federal de Uberlândia.

Defesa de: Tese de Doutorado nº 008 - COPOD

Data: 30/09/2015

Discente: Marina de Melo Naves; Matrícula: (11213ODO010)

Título do Trabalho: Características micro e macrogeométricas de implantes dentais e sua deformação no processo de instalação cirúrgica.

Área de concentração: Clínica Odontológica Integrada.

Linha de pesquisa: Implantodontia e Prótese sobre Implantes

Projeto de Pesquisa de vinculação: Implantodontia e Prótese sobre Implantes .

As **treze horas e trinta minutos** do dia **trinta de setembro do ano de 2015** no Anfiteatro Bloco 4L Anexo A, sala 23 Campus Umuarama da Universidade Federal de Uberlândia, reuniu-se a Banca Examinadora, designada pelo Colegiado do Programa de Pós-graduação em maio de 2015, assim composta: Professores Doutores: Paulo César Simamoto Júnior (UFU); Luis Henrique Araújo Raposo (UFU); César Bataglion (FORP/USP); Wilson Matsumoto (FORP/USP); Denildo de Magalhães (UFU) orientador(a) do(a) candidato(a) **Marina de Melo Naves**.

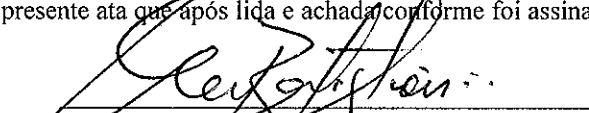
Iniciando os trabalhos o(a) presidente da mesa Dr. Denildo de Magalhães apresentou a Comissão Examinadora e o candidato(a), agradeceu a presença do público, e concedeu ao Discente a palavra para a exposição do seu trabalho. A duração da apresentação do Discente e o tempo de arguição e resposta foram conforme as normas do Programa.

A seguir o senhor(a) presidente concedeu a palavra, pela ordem sucessivamente, aos(às) examinadore(a)(s), que passaram a arguir o(a) candidato(a). Ultimada a arguição, que se desenvolveu dentro dos termos regimentais, a Banca, em sessão secreta, atribuiu os conceitos finais.

Em face do resultado obtido, a Banca Examinadora considerou o(a) candidato(a) A provado(a).

Esta defesa de Tese de Doutorado é parte dos requisitos necessários à obtenção do título de Doutor. O competente diploma será expedido após cumprimento dos demais requisitos, conforme as normas do Programa, a legislação pertinente e a regulamentação interna da UFU.


Nada mais havendo a tratar foram encerrados os trabalhos às 17 horas e 05 minutos. Foi lavrada a presente ata que após lida e achada conforme foi assinada pela Banca Examinadora.



Prof. Dr. César Bataglion – FORP/USP



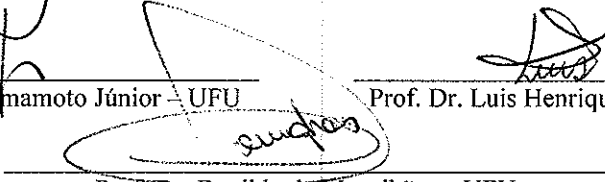
Prof. Dr. Wilson Matsumoto – FORP/USP



Prof. Dr. Paulo César Simamoto Júnior – UFU



Prof. Dr. Luis Henrique Araújo Raposo – UFU



Prof. Dr. Denildo de Magalhães – UFU
Orientador(a)



DEDICATÓRIA

Dedico este estudo à minha família, em especial: meus pais Jeová e Noélia,
marido Macarrão e irmão Marcell.

AGRADECIMENTOS ESPECIAIS

Aos meus pais, Jeová e Noélia, que são meu alicerce e referência de amor, família e segurança. Muito obrigada é muito pouco para dizer e agradecer por tudo que têm feito por mim. Amo vocês infinitamente!

Ao meu irmão Marcell, meu melhor amigo, sendo minha inspiração profissional.

Ao meu marido Macarrão, por compreender o ônus desta etapa, sendo sempre paciente e companheiro. Obrigada pelo incentivo e amor diários.

Aos meus avós, Denise, Maurílio, Guiomar e Jeová, por serem o motivo da união de nossa família e por representarem a solidez de nossa criação.

Aos meus sogros, Donato e Eleusa, cunhados (Elisa, Mariana, Carolina, Thiago, Fábio), por me receberem tão bem, proporcionando sempre bons momentos.

A Deus, por continuar guiando meus passos e abençoar minha família, meu bem mais precioso.

AGRADECIMENTOS

Ao meu orientador e amigo Prof. Dr. Denildo de Magalhães, agradeço mais uma vez os votos de confiança e todos os ensinamentos e oportunidades a mim dedicados. Obrigada por você ser quem é!

À minha co-orientadora Prof^a. Dr^a. Henara Lillian Costa, pela paciência, inteligência, eficiência e dedicação ao nosso estudo, me fazendo apaixonar cada dia mais pela engenharia mecânica. Sou fã!

Ao Prof. Ms. Helder Henrique Machado de Menezes, meu mestre e amigo, que caminha junto a nós no desenvolvimento e idealização das pesquisas, inspirando-nos na busca pelas descobertas científicas.

Aos Professores José Daniel Biasoli de Mello e Washington Martins; aos colegas Vinícius, José Lúcio e Sara; e ao LTM (FMEMC-UFU).

À Jéssica Afonso Ferreira, por participar ativamente na execução deste e outros estudos, sendo amiga e conselheira, e por me deixar participar de seu crescimento profissional.

À Universidade Federal de Uberlândia.

À Faculdade de Odontologia e à Faculdade de Engenharia Mecânica da Universidade Federal de Uberlândia

À Escola de Pós-graduação HD Ensinos Odontológicos.

Aos professores da FOUFU, em especial do Programa de Pós-graduação.

Às secretárias da Pós-graduação da FOUFU, Graça e Brenda.

À empresa Neodent pelo incentivo à pesquisa do mestrado, doutorado e em outras pesquisas.

Às amigas Anne, Carol, Vanessa, Ana Luíza, Karla Zancopé, Natália, Laura e Mari, pela doce convivência.

Aos bons amigos que tenho, e felizmente é impossível citar cada um por representarem grande número.

E a todos que foram importantes em nesta etapa.

EPÍGRAFE

Dizem que a vida é para quem sabe viver, mas ninguém nasce pronto. A vida é para quem é corajoso o suficiente para se arriscar e humilde o bastante para aprender.

(Clarice Lispector)

SUMÁRIO

Resumo.....	1
Abstract.....	2
1 Introdução e referencial teórico.....	3
2 Capítulos.....	8
Capítulo 1.....	9
Capítulo 2.....	22
Capítulo 3.....	51
3 Considerações gerais.....	58
Referências.....	59

RESUMO

A estabilidade primária e o tipo de rugosidade da superfície possui uma forte influência na osseointegração de implantes dentários. Durante a colocação do implante, danos na conexão protética e superfície do implante podem ocorrer. Devido a deformações nestas regiões dos implantes, o presente trabalho analisou os efeitos da inserção do implante em osso com o mesmo tratamento aplicado e pelo mesmo fabricante de implantes com macrogeometrias diferentes sobre parâmetros de rugosidade superficial e avaliou os níveis de deformação de conexões tipo hexágonos externo (HE) quando submetidos a torque interno. Para a análise de superfície, três grupos de implantes de titânio com diferentes macrogeometrias foram investigados usando interferometria a laser e microscopia eletrônica de varredura. Parâmetros de rugosidade superficial relevantes foram calculados para diferentes regiões de cada implante antes (B) e depois (A) da inserção em costelas de porco. Para a deformação das conexões HE, foram utilizados dois tipos de implantes (S e N) e o torque interno foi aplicado. A distância interna (ID), a área interna (IA) e externa (EA) do HE foram obtidas. Os topos de rosca de todos os implantes B obtiveram parâmetros de rugosidade muito semelhantes, independentemente da geometria do implante, e depois da inserção em osso, esta foi a região que apresentou alterações significativas. Em contraste, os flancos e vales das roscas apresentaram maiores irregularidades (S_a), com maiores inclinações (S_dq) em todos os implantes B, especialmente para implantes com altura de rosca menor. Os níveis de deformação do HE foram maiores no grupo S (SIN), em comparação com o grupo N (Neodent). Este estudo preliminar demonstrou danos na superfície dos implantes após o processo de instalação do implante pelas mudanças observadas nos parâmetros de rugosidade, afetados pela macrogeometria e o HE pode ser afetado por diferentes níveis de torque interno.

Palavras-chave: implantes dentários, topografia de superfície, conexão protética.

ABSTRACT

Primary stability and the type of surface roughness have a strong influence on the dental implants osseointegration. During implant placement, damage on the prosthetic connection and implant surface may occur. Due to the deformations in this portion of the implants, this work analyzed the effects of implant insertion into bone on the surface roughness parameters for the same surface treatment applied by the same manufacturer to implants with different macro-designs and evaluated the levels of deformation in external hexagon (EH) connections subjected to internal torque. For the surface analysis, three groups of titanium implants with different macro-designs were investigated using laser interferometry and scanning electron microscopy. Relevant surface roughness parameters were calculated for different regions of each implant before (B) and after (A) insertion into pork ribs. For the deformation of EH connections, two types of implants (S and N) were used and internal torque were applied. The internal distance (ID), internal area (IA) and external area (EA) of the EH were obtained. The tops of the threads of all B implants had very similar roughness parameters, independent of the geometry of the implant, after bone insertion, this was the region that presented significant alterations. In contrast, the flanks and valleys of the threads presented larger irregularities (S_a) with higher slopes (S_dq) on all B implants, particularly for implants with threads with smaller heights. Levels of EH deformation were greater in the S group as compared with the N group. This preliminary study demonstrated surface damage of the implants after the installation process by the changes observed on roughness parameters, which were affected by the macrogeometry. The EH may be affected by different internal torque levels.

Key words: dental implants, surface topography, abutment connection.

1. INTRODUÇÃO E REFERENCIAL TEÓRICO

A interação íntima entre implante e osso (osseointegração) (Brånemark et al., 1969) fez dos implantes dentais uma das modalidades de reabilitação de mais sucesso no campo da saúde, com taxas de sucesso frequentemente excedendo 95% por muitos anos (Chuang & Cai 2006; Levine et al. 2002; Zupnik et al. 2011). Ainda assim, pesquisa e desenvolvimento no campo da Implantodontia são focados com frequência no redesenho do implante (por exemplo, conexão, topografia, superfície, macrodesenho) para continuar melhorando as taxas de sucesso.

Novos desenhos de implantes buscam aperfeiçoar resultados em situações propícias a falhas, como baixa densidade óssea dos maxilares ou pacientes com doenças sistêmicas que comprometem a cicatrização. Esses emergentes desenvolvimentos são baseados, por exemplo, na modificação química ou mecânica do implante. Tais modificações objetivam melhorar a resposta do hospedeiro e acelerar o processo de cicatrização.

Achados clínicos sugerem que essas modificações, particularmente no tipo de superfície, têm ajudado a aumentar a taxa de sucesso de implantes dentais (Trisi et al. 2003). Uma série de eventos coordenados que incluem proliferação celular, transformação de osteoblastos, e formação de tecido ósseo podem ser afetados por diferentes topografias de superfície (Shibli et al. 2007). A quantidade de contato osso implante é um fator determinante para o sucesso a longo prazo de implantes dentais. Consequentemente, a maximização desse contato e a osseointegração tornaram-se um dos focos do tratamento, que aparentemente pode ser aumentada por meio da variação de rugosidade da superfície do implante (Soskolne et al., 2002). Avaliações demonstraram que implantes com superfícies rugosas mostram melhor aposição óssea e contato osso-implante que implantes com superfícies lisas (Buser et al. 1999; Buser et al., 1991). A rugosidade superficial também tem influência na migração e proliferação celular que, em partes, leva ao melhor contato osso-implante, sugerindo que a microtopografia de implantes de titânio influencia na interação tecido-biomaterial (Abron et al., 2001; Novaes et al.,

2002). A quantificação precisa da superfície de um implante é necessária para analisar os efeitos dessa microtopografia nos resultados tanto da osseointegração quanto do contato osso-implante.

A avaliação quantitativa da topografia de superfície pode ser realizada utilizando instrumentos com métodos de contato mecânico (perfilometria, microscópio de força atômica) ou instrumentos ópticos (interferometria óptica) (Wennerberg & Albrektsson, 2000). Implantes do tipo parafuso contêm roscas com vales profundos, que torna a avaliação por perfilometria de contato difícil (Kilpadi & Lemons, 1994; Vercaigne et al., 1998). Microscopia de força atômica pode detectar alterações topográficas ao nível do tamanho de uma molécula de proteína, mas é limitada a uma pequena área, o que pode não ser representativo para a área total do implante (Wennerberg & Albrektsson, 2000). Instrumentos ópticos (Bennett & Mattsson, 1999; Dong et al., 1994a) não envolvem contato mecânico, mas os resultados são menos confiáveis quando são feitas medições em superfícies que apresentam inclinações maiores que 15 graus.

Após a aferição da superfície do implante, diferentes parâmetros podem ser calculados para quantificar sua topografia. O guia 428717 da Organização Internacional de Padronização (ISO) define parâmetros bidimensionais (2D), e parâmetros tridimensionais (3D) são extrapolações dos seus homólogos 2D. Embora os parâmetros de rugosidade 3D ainda não tenham sido inclusos no padrão ISO, eles são bem conhecidos e descritos na literatura (Stout et al., 1993; Dong et al., 1993; Dong WP, et al., 1994b).

Para implantes dentais, diversos parâmetros devem ser avaliados: três parâmetros de altura (rugosidade média aritmética [S_a], distribuição da altura de picos da topografia, também conhecido como Kurtosis [S_{ku}], e a assimetria da altura de topografia [S_{sk}]); um parâmetro espacial (relação do aspecto de textura superficial [S_{tr}]); e dois parâmetros híbridos (raiz média quadrática dos picos de superfície [S_{dq}] e relação do aumento da área [S_{dr}]).

Alterações na macrogeometria do implante, com relação ao formato, também podem contribuir para o sucesso do implante dental, afetando diretamente na estabilidade primária (Coelho et al., 2011; Deporter D, 2009;

Degidi & Piattelli, 2005). Resultados na literatura (Javed & Romanos, 2010) sugerem que os torques de inserção de implantes cônicos são maiores que em implantes cilíndricos. Este comportamento pode ser atribuído às diferenças no formato de rosca, geometria do implante e área de superfície. A geometria das roscas desses implantes cônicos significa que uma maior área da superfície está em contato com tecido do hospedeiro (Elias et al., 2012). Portanto, o melhor desenho do implante deve ser selecionado para uma instalação em sítios críticos a fim de melhorar a estabilidade primária. As características macrogeométricas do implante dental, particularmente padrão e passo de rosca, podem ser responsáveis por diferenças na quantidade de osso que circunda o implante e no grau de aposição óssea (por exemplo) nas roscas achatadas versus roscas afiladas, e seu impacto no sucesso da estabilização e manutenção da osseointegração do implante (Cardoso et al., 2013).

Foi demonstrado que a rugosidade de superfície pode variar de acordo com sua localização no implante (Naves et al., 2015). Além disso, em implante do tipo parafusado é necessário que a medida de topografia de superfície seja realizada em três regiões da rosca: flanco, topo e fundo (Wennerberg & Albrektsson 2000; Gonçalves et al., 2012; Rosa et al., 2013). Recentemente, Rosa et al. (2012) mostraram que quando o mesmo método de modificação superficial é aplicado a implantes de titânio produzidos por diferentes fabricantes, a rugosidade final pode ser significativamente diferente. Além disso, o tratamento de superfície por si só não pode determinar a topografia de superfície final dos implantes. Entretanto os autores não analisaram com detalhes a razão dessa diferença.

A estabilidade primária também é considerada o fator chave para o prognóstico da osseointegração (Duyck et al., 2015). O carregamento imediato requer alta estabilidade primária (Rea et al., 2015) que pode ser medida pelo valor do torque aplicado durante a instalação cirúrgica do implante (Barikani et al., 2014; Shokri & Daraeighadikolaei, 2013). É sabido que a alta estabilidade primária diminui a micromovimentação dos implantes dentários e melhora a interface osso-implante (Alsaadi et al., 2007; Fanuscu et al., 2007; Irinakis & Wiebe, 2009; Maeda et al., 2006). O controle de torque além de fácil de aplicar

e é disponível, tornando-se um excelente parâmetro clínico para esta estabilidade. Valores maiores que 35 N.cm são considerados aceitáveis. Este valor pode ser determinado durante a perfuração e fixação cirúrgica do implante, por meio de um torquímetro pré-calibrado (Alsaadi et al., 2007; Fanuscu et al, 2007; Maeda et al., 2006; Neugebauer et al., 2009).

A obtenção de uma boa estabilidade primária depende de alguns fatores, como características macrogeométricas, como formato de rosca e diâmetro, o uso de técnicas de compressão óssea, habilidade e experiência do cirurgião ao identificar a densidade óssea para escolher brocas finais (Alsaadi et al., 2007; Irinakis & Wiebe, 2009; Sakoh et al., 2006a; Trisi et al., 2009). Quando estes fatores estão presentes de maneira favorável, situação não muito frequente, é possível alcançar alta estabilidade, demandando altos níveis de torque e tornando a instalação do implante difícil. Os adaptadores convencionais usados para carregar o implante até o alvéolo de inserção e rosquear o implante têm sido gradativamente substituídos por adaptadores ou chaves com conexões internas diferentes. Estes sistemas utilizam do contato interno com as paredes do implante ao invés de montadores para aplicar a força, o que simplifica o procedimento e diminui o custo do material. No entanto, os mecanismos do sistema sempre atingirão um limite de resistência, e torque excessivo pode causar danos à estrutura cervical do implante e à conexão protética (Alsaadi et al., 2007; Sakoh et al., 2006b).

Diante das possíveis alterações micro e macrogeométricas nos implantes dentais, este estudo analisou a hipótese que certo tipo de modificação de superfície, quando aplicado a diferentes macrogeometrias de implantes, pode resultar em padrões de rugosidade superficial diferentes, mesmo se todas as modificações são produzidas pelo mesmo fabricante, e tal superfície pode sofrer alterações no processo de instalação cirúrgica do implante dental. Além disso, a aplicação de torque interno neste mesmo processo de inserção do implante pode resultar em danos geométricos na conexão do tipo hexágono externo.

Assim, o objetivo deste estudo foi caracterizar a topografia de superfície de três implantes comercialmente disponíveis com diferentes

macrogeometrias, produzidos pelo mesmo fabricante, que tiveram suas superfícies modificadas pelo processo de jateamento e ataque ácido. Esta caracterização incluiu parâmetros de altura, espaço e funcionalidade de rugosidade e analisou o efeito da macrogeometria nestes parâmetros, antes e após o procedimento de inserção óssea. Adicionalmente, objetivou-se avaliar *in vitro* os níveis de deformação de conexões hexágono externo de dois sistemas diferentes submetidas ao torque interno.

2. CAPÍTULOS

CAPÍTULO 1

EFFECT OF THE MACROGEOMETRY ON THE SURFACE TOPOGRAPHY OF DENTAL IMPLANTS

Naves MM, Menezes HH, Magalhães D, Ferreira JA, Ribeiro SF, de Mello JD, Costa HL. Effect of Macrogeometry on the Surface Topography of Dental Implants.

Int J Oral Maxillofac Implants. 2015 Jul-Aug;30(4):789-99.

Effect of Macrogeometry on the Surface Topography of Dental Implants

Marina Melo Naves, MSc¹/Helder Henrique Machado Menezes, MSc²/
Denildo Magalhães, PhD³/Jessica Afonso Ferreira, BS⁴/Sara Ferreira Ribeiro, BIng⁵/
José Daniel Biasoli de Mello, Dr Ing⁶/Henara Lillian Costa, PhD⁷

Purpose: Because the microtopography of titanium implants influences the biomaterial-tissue interaction, surface microtexturing treatments are frequently used for dental implants. However, surface treatment alone may not determine the final microtopography of a dental implant, which can also be influenced by the implant macrogeometry. This work analyzed the effects on surface roughness parameters of the same treatment applied by the same manufacturer to implants with differing macro-designs. **Materials and Methods:** Three groups of titanium implants with different macro-designs were investigated using laser interferometry and scanning electron microscopy. Relevant surface roughness parameters were calculated for different regions of each implant. Two flat disks (treated and untreated) were also investigated for comparison. **Results:** The tops of the threads and the nonthreaded regions of all implants had very similar roughness parameters, independent of the geometry of the implant, which were also very similar to those of flat disks treated with the same process. In contrast, the flanks and valleys of the threads presented larger irregularities (Sa) with higher slopes (Sdq) and larger developed surface areas (Sdr) on all implants, particularly for implants with threads with smaller heights. The flanks and valleys displayed stronger textures (Str), particularly on the implants with threads with larger internal angles. **Conclusion:** Parameters associated with the height of the irregularities (Sa), the slope of the asperities (Sdq), the presence of a surface texture (Str), and the developed surface area of the irregularities (Sdr) were significantly affected by the macrogeometry of the implants. Flat disks subjected to the same surface treatment as dental implants reproduced only the surface topography of the flat regions of the implants. INT J ORAL MAXILLOFAC IMPLANTS 2015;30:789–799. doi: 10.11607/jomi.3934

Key words: dental implants, implant design, osseointegration, surface texturing, surface topography, titanium

¹PhD Candidate, School of Dentistry, Universidade Federal de Uberlândia, Campus Umuarama, Uberlândia, Brazil; HD Ensinos Odontológicos, Uberlândia, Brazil.

²Lecturer, HD Ensinos Odontológicos, Uberlândia, Brazil.

³Professor, School of Dentistry, Universidade Federal de Uberlândia, Campus Umuarama, Uberlândia, Brazil; HD Ensinos Odontológicos, Uberlândia, Brazil.

⁴Student, School of Dentistry, Universidade Federal de Uberlândia, Campus Umuarama, Uberlândia, Brazil.

⁵Student, Laboratory of Tribology and Materials, Universidade Federal de Uberlândia, Campus Sta. Monica, Uberlândia, Brazil.

⁶Professor, Laboratory of Tribology and Materials, Universidade Federal de Uberlândia, Campus Sta. Monica, Uberlândia, Brazil.

⁷Associate Professor, Laboratory of Tribology and Materials, Universidade Federal de Uberlândia, Campus Sta. Monica, Uberlândia, Brazil.

Correspondence to: Henara Lillian Costa, Laboratory of Tribology and Materials, Universidade Federal de Uberlândia, Campus Sta. Monica, Bl. 5K 38400-901, Uberlândia, Brazil. Fax: +55-3432394273. Email: ltm-henara@ufu.br

©2015 by Quintessence Publishing Co Inc.

The close interaction between bone and implants (osseointegration)¹ has made dental implants one of the most successful rehabilitation modalities in the medical field, with success rates often exceeding 95% over a number of years.^{2–4} Yet, research and development in the field of implant dentistry are frequently focused on implant redesign (eg, topography, implant surface, macro-design) to continue improving implant success rates. Newer implant designs seek to address situations that are prone to failure, such as jawbone with low density or patients with systemic diseases that compromise healing. Emerging new developments are based, for example, on modification of either the chemical or the mechanical properties of an implant. They are expected to improve the host tissue response and to accelerate the healing process. Clinical findings suggest that these changes, particularly in implant surface design, have helped increase dental implant success.⁵

The series of coordinated events that includes cell proliferation, transformation of osteoblasts, and bone tissue formation might be affected by different surface topographies.⁶ The amount of bone-to-implant contact (BIC) is an important determinant in the long-term success of dental implants. Consequently, maximization of BIC and osseointegration has become a goal of treatment, which apparently can be enhanced by varying the roughness of the implant surface.⁷ Evaluations have demonstrated that implants with rough surfaces show better bone apposition and BIC than implants with smooth surfaces.^{8,9} Surface roughness also has a positive influence on cell migration and proliferation, which in turn leads to better BIC, suggesting that the microtopography of titanium implants influences the biomaterial-tissue interaction.^{10,11}

Precise quantification of an implant's surface roughness is necessary to analyze the effects of its microtopography on such outcomes as BIC and osseointegration. A quantitative evaluation of surface topography can be carried out using instruments with mechanical contact methods (profilometry, atomic force microscopy) or optical instruments (optical interferometry).¹² Screw-type implants contain threads with deep valleys, which makes evaluation by contact profilometry difficult.^{13,14} Although mechanical styluses often have a measuring range in the vertical direction of several millimeters, it may be impossible to reach the valley and flank areas because of the size of the tip, the presence of the cantilever, and the small pitch height of the threads of a dental implant. Atomic force microscopy can detect changes in the range of a protein molecule size, but it is limited to a small area, which may not be representative of the total implant area.¹² Optical instruments^{15,16} do not involve mechanical contact, but the results are less reliable when surfaces with slopes greater than 15 degrees are measured.

After the implant's surface is assessed, different parameters can be calculated to quantify its topography. International Organization for Standardization (ISO) guideline 4287¹⁷ defines two-dimensional (2D) roughness parameters, and 3D roughness parameters are extrapolations of their 2D counterparts. Although 3D roughness parameters have not yet been included in the ISO standards, they are well known and described in the literature.¹⁸⁻²⁰

For dental implants, several parameters should be evaluated: three height parameters (arithmetic mean roughness [Sa], peakedness of the topography height distribution, also known as kurtosis [Sku], and skewness of topography height distribution [Ssk]); one spatial parameter (texture aspect ratio of the surface [Str]); and two hybrid parameters (root-mean-square slope of the surface [Sdq] and developed interfacial area ratio [Sdr]).

Changes in implant macrogeometry have also contributed to implant success, directly affecting primary stability.²¹⁻²³ Results in the literature²⁴ suggest that the insertion torque of conical implants is higher than that of cylindrical implants. This behavior can be attributed to differences in thread shape, implant geometry, and surface area. The thread geometry of conical implants means that a larger surface area is in contact with the host tissue.²⁵ Thus, the best dental implant design may be chosen for its placement in critical sites to improve primary stability. Dental implant macro-design features, particularly thread pattern and thread pitch, can be responsible for differences in the amount of bone surrounding the implant and in the degree of bone apposition onto (for example) buttress threads versus V-threads, and they may impact the success of the establishment and/or maintenance of implant osseointegration.²⁶

It has been shown that surface roughness can vary according to its location on the implant. Therefore, in screw-type implants it is necessary to measure surface topography in three regions of the threads: flank, top, and bottom.^{12,27,28}

Recently, Rosa et al²⁹ showed that when the same surface modification method is applied to titanium implants produced by different manufacturers, the final surface roughness can be significantly different. Therefore, surface treatment alone cannot determine the final surface topography of implants. However, the authors did not analyze in detail the reason for this difference.

This paper analyzes the hypothesis that a certain type of surface modification, when applied to implants with different macrogeometries, can result in different surface roughness parameters, even if all implants and modifications are produced by the same manufacturer. Particular attention must be paid to different regions of the screw (bottom, top, and flank) because of the different angles between the regions to be treated and the source used to modify the surface, most often a jet used for particle blasting.

Therefore, the aim of this study was to characterize the surface topography of three commercially available titanium implants with different macrogeometries, produced by the same manufacturer, which had their surface modified by a process that includes sand-blasting and acid etching. This characterization included height, spacing, and functional surface roughness parameters and assessed the effect of the macrogeometry of the implants on those parameters. In addition, for comparison, measurements were carried out on flat disks that received the same surface treatment, since *in vitro* studies to characterize cell growth as a function of the surface treatment applied to an implant are typically carried out on flat disks.²⁹

MATERIALS AND METHODS

Description of the Samples

This study investigated three groups (Alvim, Drive, and Titamax EX) of bone-compacting, commercially pure (grade 4) titanium implants produced by the same company (Neodent). Compacting-type implants were chosen because they present a conical or hybrid design, where the apical region is narrower than the cervical region. All implants featured a Morse taper connection and had a diameter of 3.5 mm and a length of 13 mm. However, they presented different macrogeometries, as shown in Fig 1. Three samples of each implant type were assessed.

The surface modification applied to all implants was identical and was a trademark of the company (Neoporos, Neodent). The surface modification method consists of, first, blasting using abrasive particles with automated control of the velocity, direction, pressure, and size of particles. In sequence, aluminum oxide particles of controlled size create craters on the surface of the implant. Finally, acid etching is used to ensure uniform surface topography.

For comparison, two types of flat disks were also prepared by Neodent. The disks were 6 mm in diameter and 2 mm high. The first flat disk received the same Neoporos surface treatment to determine whether the treatment applied to the flat surfaces was the same as when it was applied to surfaces with different geometries. The second was a disk with a smooth surface obtained by conventional polishing. This was measured to verify whether any region of any implant would have surface roughness parameters identical to those of the smooth disk, which would indicate that the region was not affected at all by the surface treatment applied.

Surface Characterization

Laser interferometry and scanning electron microscopy (SEM) were used for surface characterization of the implants and disks. A 3D laser interferometer (UBM MESSTECHNIK MicroFocus) was used to assess the surface topography of the dental implants. Measurement densities of $1,000 \times 1,000$ points were used. The measuring rate was 300 points/s, and continuous measurement mode was used. The measurement area (0.8×0.4 mm) was chosen so that it could include at least one thread for all the regions without losing focus.

Because the implants featured complex macrogeometry, different areas were measured for each implant, as exemplified in Fig 2. There were 11 samples: three Drive implants, three Alvim implants, three Titamax EX implants, one Neoporos disk, and one smooth disk. Each implant was divided into three regions (cervical [1], middle body [2], and apical [3]) (Fig 2a). In addition, the nonthreaded area of each implant was also

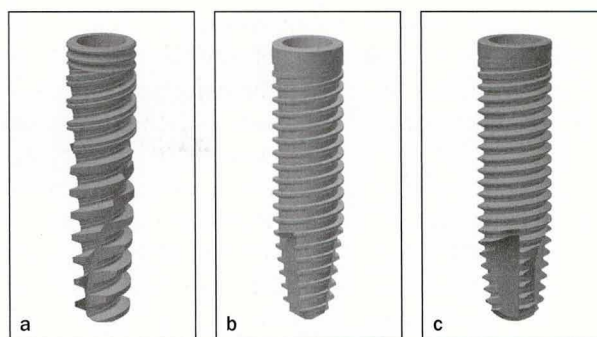


Fig 1 Macrogeometry of each implant tested. (a) Drive, (b) Alvim, (c) Titamax EX.

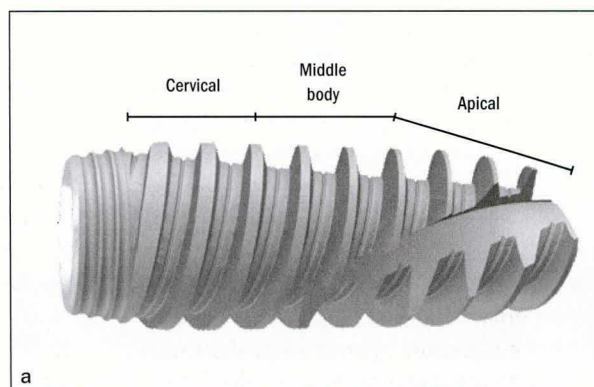


Fig 2a Regions of analysis of the implants.

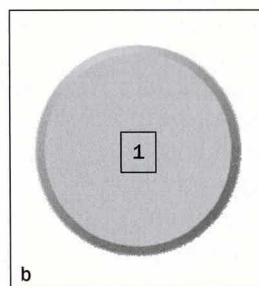


Fig 2b Region of analysis of the disks.

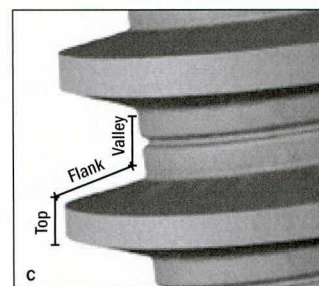


Fig 2c Areas analyzed in regions 1, 2, and 3.

measured [4]. Then, for each region (cervical, middle body, and apical), three consecutive thread tops, three consecutive thread valleys, and three consecutive thread flanks were measured separately (Fig 2c). Three regions with the same dimensions (0.8×0.4 mm) in the nonthreaded area were also measured, for a total of 30 measurements per implant.

For the flat disks, three regions with dimensions of 0.8×0.4 mm were randomly chosen on the top of the disk surface (Fig 2b).

Surface topography characterization consists of three components: form, waviness, and roughness.

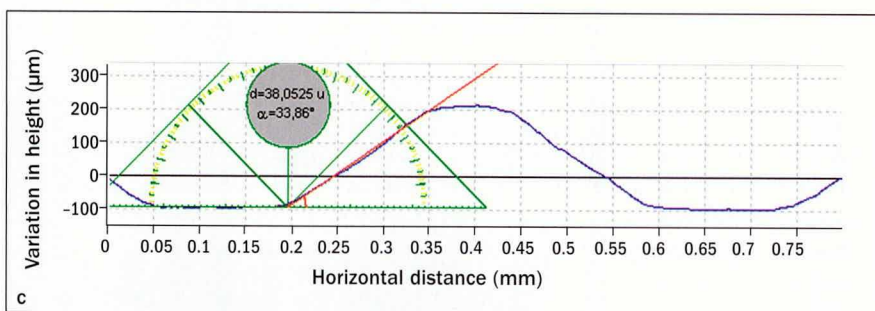
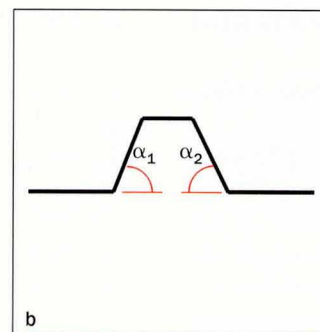
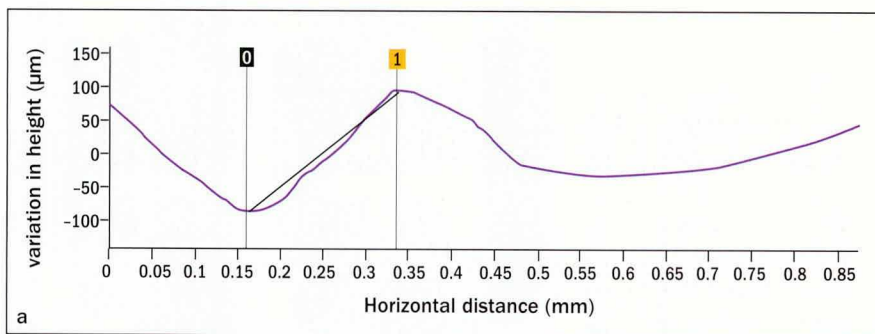


Fig 3 Parameters measured to characterize the macrogeometry of the implants. (a) Thread height. (b) Thread angles. (c) Scheme for angle measurement in threads with complex shape.

Table 1 Macrogeometric Measurements of the Implants

Implant/region	α_1 (deg)	α_2 (deg)	h (µm)
Drive			
Region 1	45.0	66.0	104
Region 2	46.3	38.5	149
Region 3	52.3	43.5	157
Mean	48.6		137
Alvim			
Region 1	37.3	27.2	223
Region 2	43.9	43.5	184
Region 3	59.4	37.1	138
Mean	41.4		182
Titamax EX			
Region 1	18.8	17.4	212
Region 2	35.8	33.2	238
Region 3	29.0	43.6	162
Mean	29.6		204

For topographic evaluation, it is necessary to separate these components using filters. After form removal, a filtering process separated waviness and surface roughness. It used a 50- × 50-µm Gaussian filter, according to ISO 11562 recommendations.³⁰

To characterize the macrogeometry of the implants, profiles of the threads were selected after form removal (Fig 3). MountainsMap software (Digital Surf) was used for this purpose, and it also provided visual 2D and 3D images of the surfaces and numeric descriptions of

their surface roughness parameters. Vertical heights (Fig 3a) and angles (Fig 3b) of the threads were measured to quantify the macrogeometry of each implant. When the geometry of the thread was complex, the software MB Ruler (Markus Bader MB Software Solutions) was used to calculate the angles (Fig 3c).

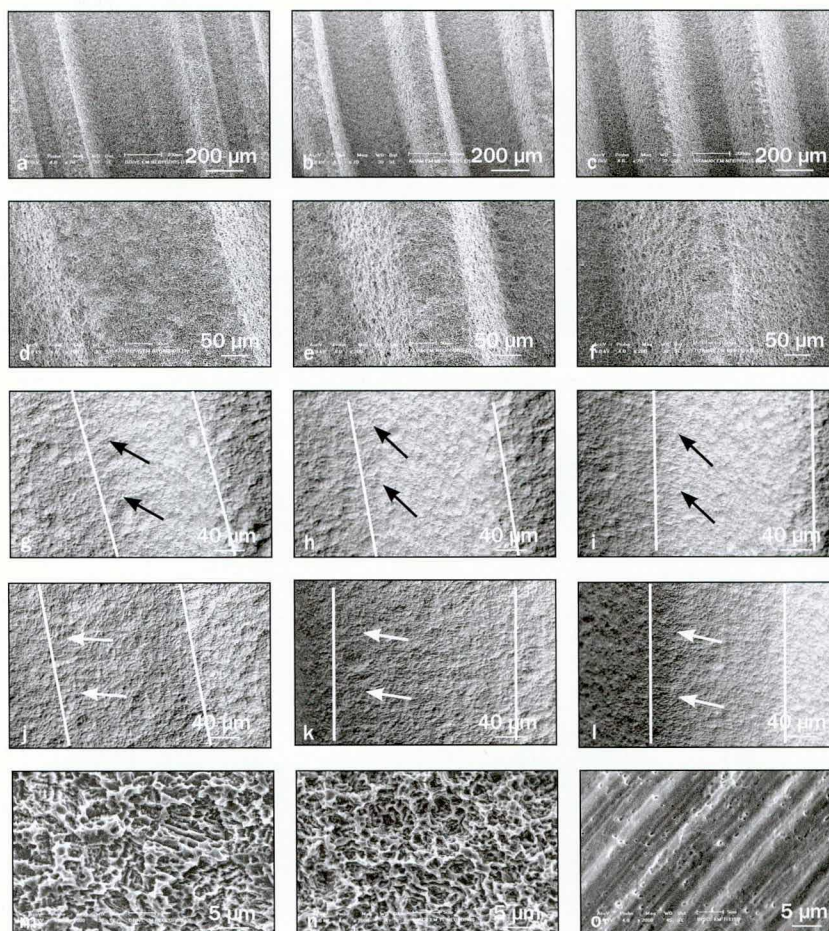
The numeric description of the surface roughness of the implants in the different regions of the threads and in the flat regions of the implants and disks used the following roughness parameters: Sa, Ssk, Sku, Str, Sdq, and Sdr, as suggested by Wennerberg and Albrektsson.¹² Mathematic descriptions of those parameters can be found in Stout et al.¹⁸

SEM imaging of the tops, flanks, and valleys of the threads; of the unthreaded areas for the implants; and of the flat disks was carried out to provide a qualitative analysis of the surfaces (EVO MA 10, Carl Zeiss) under different magnifications and an acceleration voltage of 15 kV.

Statistical Analysis

Statistical analysis at a 95% level of significance was performed via analysis of variance using a factorial scheme with one additional treatment (the nonthreaded areas of each implant) and one control treatment (the sandblasted acid-etched flat titanium disks). The factors used were the regions (1, 2, 3, and 4), the areas (top, flank, and valley) and the macrogeometries of the implants. After the normality of the data distribution was verified, the Scott-Knott test³¹ was used to compare factorial treatment means, and the Dunnett and Tamhane test³² was used to compare the control treatment with the other factorial treatments.

Fig 4 SEM images of the implants. (a) Drive, general view; (b) Alvim, general view; (c) Titamax EX, general view; (d) Drive, top; (e) Alvim, top; (f) Titamax EX, top; (g) Drive, flank; (h) Alvim, flank; (i) Titamax EX, flank; (j) Drive, valley; (k) Alvim, valley; (l) Titamax EX, valley; (m) zoom showing a typical top; (n) Neoporos flat disk; (o) smooth flat disk. White lines delimit the areas of interest, and arrows indicate direction of texture.



RESULTS

Table 1 presents the values for the parameters used to characterize the threads in the three different regions of each implant. Some variation in the angles and heights between the different regions of the same implant was apparent. The Drive implant tended to present threads with smaller heights, whereas the implant Titamax EX tended to present threads with smaller external angles.

The top row of Fig 4 shows global images of all the implants at low magnifications. When the tops of the threads were viewed under high magnification, the morphology of all implants appeared very similar. When intermediate magnifications (additional rows) were used to investigate individually each part of the threads (top, flank, valley), some directionality was seen for all the flanks (*third row, g, h, and i*) and for most valleys (*fourth row, j and k*). Arrows were added to the images to indicate the direction of texture, and lines were added to limit the region under discussion. Also, those regions appeared rougher than the tops (*d, e,*

and f). The morphology of the Neoporos flat disk under high magnification (*n*) was similar to that observed for the tops of the threads (*m*). On the other hand, the morphology of the smooth disk (*o*) was very different from those of both the Neoporos flat disk and any region of the implants.

Figure 5 shows 3D maps of the different regions measured on the Drive dental implant after the removal of form and waviness. This figure emphasizes the differences in the morphology of the surfaces between regions 1, 2, and 3 of the implant (compare horizontally) and between the top, flank, and valley of each region (compare vertically). Similar differences were observed for the Alvim dental implant (Fig 6) and the Titamax EX dental implant (Fig 7). Figure 8 presents 3D maps for the flat disks with both treated and smooth surfaces.

The mean values \pm standard deviations of the surface roughness parameters (Sa, Ssk, Sku, Str, Sdq, and Sdr) were averaged along regions 1, 2, and 3 of each type of dental implant and are shown in Table 2. This table also shows mean values of the surface roughness parameters for the nonthreaded regions of each

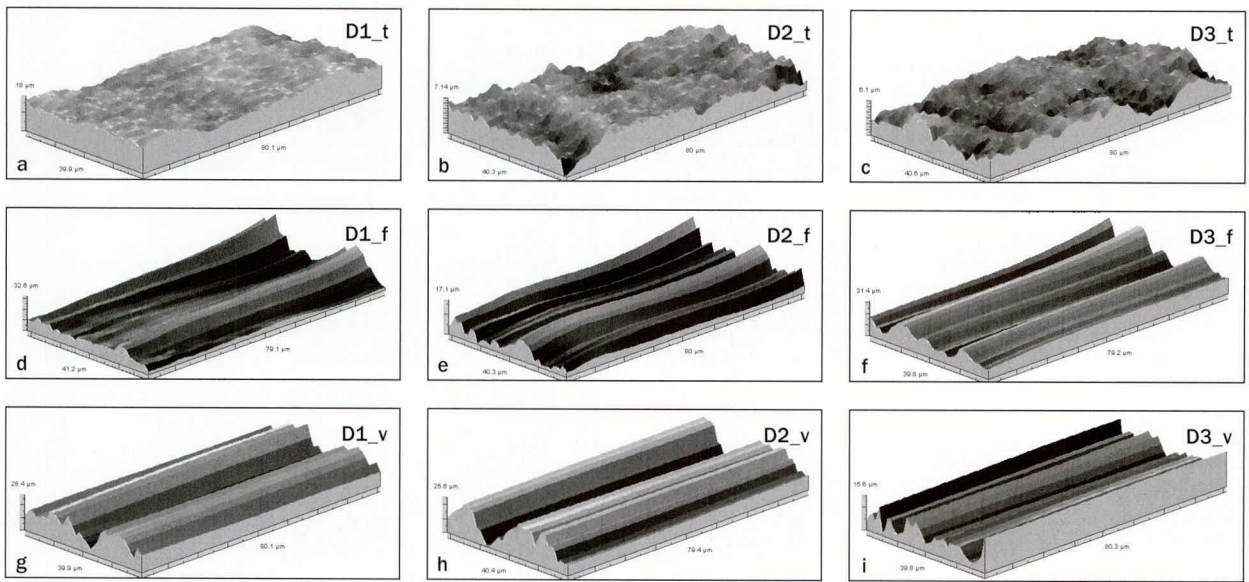


Fig 5 Three-dimensional interferometric maps for Drive implant. (a) D1_t = region 1, top; (b) D2_t = region 2, top; (c) D3_t = region 3, top; (d) D1_f = region 1, flank; (e) D2_f = region 2, flank; (f) D3_f = region 3, flank; (g) D1_v = region 1, valley; (h) D2_v = region 2, valley; (i) D3_v = region 3, valley.

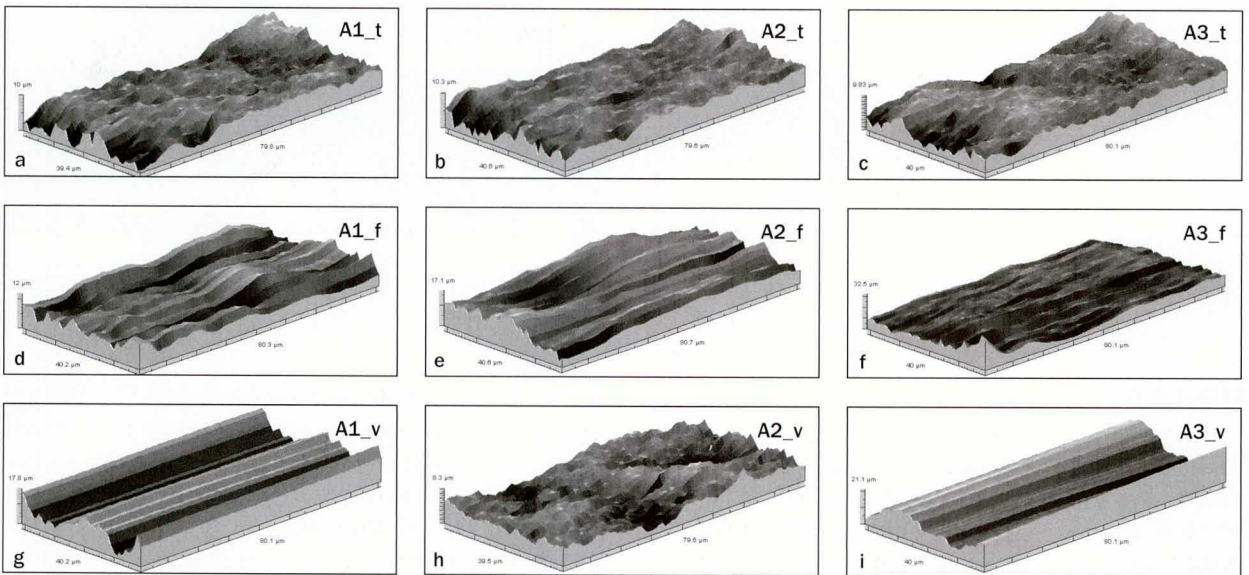


Fig 6 Three-dimensional interferometric maps for Alvim implant. (a) A1_t = region 1, top; (b) A2_t = region 2, top; (c) A3_t = region 3, top; (d) A1_f = region 1, flank; (e) A2_f = region 2, flank; (f) A3_f = region 3, flank; (g) A1_v = region 1, valley; (h) A2_v = region 2, valley; (i) A3_v = region 3, valley.

implant and disk. Table 2 shows that for the non-threaded regions and the tops of the threads, the average height deviation (Sa) was very similar between the different implant designs. Moreover, the values of the Neoporos flat disk and the tops of the threads (ie, non-threaded areas) were very similar. On the other hand, all the flanks and valleys presented higher values for Sa than the nonthreaded regions and the tops of the threads. Another important observation is that, for the valleys and flanks of the threads, the dental implant

macrogeometry had a strong effect on Sa. Finally, the values of Sa for the smooth disks were smaller than for all regions of all implants.

The parameters associated with the distribution of the heights of the deviations are Ssk and Sku. All the regions of all implants showed Ssk values close to 0 and values of Sku close to 3. Also, no significant difference between the values of Ssk and Sku for different implants and different regions was found from the statistical analysis.

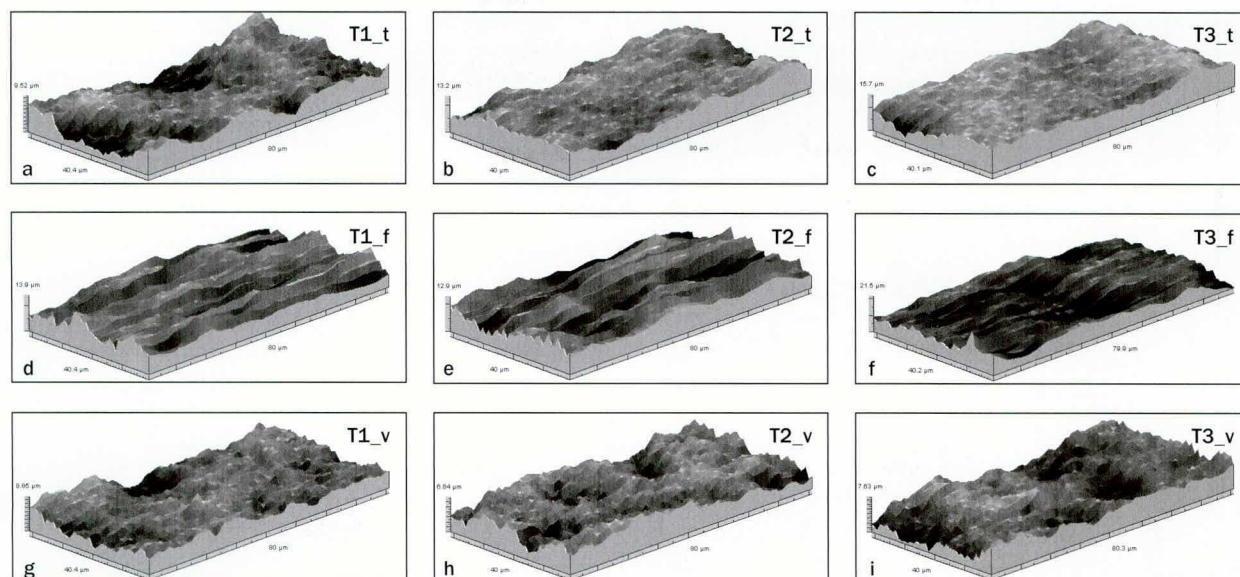
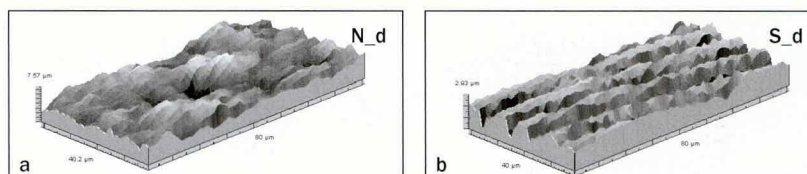


Fig 7 Three-dimensional interferometric maps for Titamax EX implant. (a) T1_t = region 1, top; (b) T2_t = region 2, top; (c) T3_t = region 3, top; (d) T1_f = region 1, flank; (e) T2_f = region 2, flank; (f) T3_f = region 3, flank; (g) T1_v = region 1, valley; (h) T2_v = region 2, valley; (i) T3_v = region 3, valley.

Fig 8 Three-dimensional interferometric maps for the titanium flat disks. (a) N_d = Neoporos disk; (b) S_d = smooth disk.



To quantify texture strength, ie, the uniformity of the texture, the parameter *Str*, which assesses the texture aspect ratio of the surfaces, was measured, and the results are shown in Table 2. All implants showed smaller values for *Str* in the flanks and valleys of the threads than the tops, which suggests a stronger directionality. These values corroborate the visual images provided by the 3D maps (Fig 6). One exception is the valleys of the threads for Titamax EX implants, which showed *Str* values similar to those at the tops of the threads, which confirms the visual indication of more uniform textures in these regions when compared with the flanks.

The values of *Sdq*, which represent the root-mean-square values of the slopes of the asperities, are also shown in Table 2. The tops of the threads and the non-threaded regions showed similarities in this parameter, independent of the macrogeometry of the implant. The flanks and valleys of the threads showed asperities that are more inclined. The largest and most scattered values for *Sdq* were found for the flanks and valleys of the Drive implant.

The values of *Sdr* were higher for the flanks and valleys, and the largest and most scattered *Sdr* values were seen for the Drive implant.

The results shown in Table 2 show the average results of the surface roughness parameters for regions 1, 2, and 3 distinguished according to macrogeometry (Alvim, Drive, Titamax EX) and the portion of the thread (top, flank, or valley). The parameters associated with the distribution of the heights of the asperities (*Ssk* and *Sku*) were not significantly different, independent of the geometry of the implant, of the region within each implant, and of the portion of the thread (top, flank, or valley). For all other parameters, the differences between the geometry and between the portion of the thread (top, flank, valley) were more significant than the differences between regions, as exemplified in Tables 3 and 4 for the parameters *Sa* and *Sdq*.

The factorial analyses shown in Tables 3 and 4 used the regions of analysis of the implants (1: cervical, 2: middle body, 3: apical) as Factor A; the portion of the thread (1: flank, 2: valley, 3: top) as Factor B; and the implant designs (1: Alvim, 2: Drive, 3: Titamax EX) as

Table 2 Surface Roughness Parameters at Four Different Sites on Commercial Screw-type Implants and Flat Disks Obtained Using Laser Interferometry

	Top	Flank	Valley	Nonthreaded area	Total	Neoporos disk	Smooth disk
Sa							
Drive	0.24 ± 0.04 ^{Aa}	1.15 ± 0.45 ^{Ba}	1.23 ± 0.67 ^{Ba}	0.25 ± 0.02 ^{Aa}	0.81 ± 0.64 [†]	0.28 ± 0.01 ^{A†}	0.15 ± 0.01 ^{DS}
Alvim	0.26 ± 0.04 ^{Aa}	0.69 ± 0.13 ^{Bb}	0.54 ± 0.21 ^{Cb}	0.26 ± 0.03 ^{Aa}	0.47 ± 0.23 [†]		
Titamax EX	0.28 ± 0.02 ^{Aa}	0.73 ± 0.14 ^{Bb}	0.33 ± 0.04 ^{Ac}	0.27 ± 0.01 ^{Aa}	0.43 ± 0.21 [†]		
Sq							
Drive	0.31 ± 0.05 ^{Aa}	1.45 ± 0.57 ^{Ba}	1.58 ± 0.90 ^{Ba}	0.32 ± 0.02 ^{Aa}	1.03 ± 0.83 [†]	0.35 ± 0.01 ^{A†}	0.18 ± 0.02 ^{DS}
Alvim	0.34 ± 0.06 ^{Ab}	0.86 ± 0.16 ^{Bb}	0.69 ± 0.27 ^{Cb}	0.33 ± 0.04 ^{Aa}	0.60 ± 0.29 [†]		
Titamax EX	0.36 ± 0.02 ^{Aa}	0.95 ± 0.13 ^{Bb}	0.43 ± 0.05 ^{Ac}	0.35 ± 0.01 ^{Aa}	0.56 ± 0.27 [†]		
Ssk							
Drive	0.06 ± 0.16 [*]	-0.01 ± 0.40 [*]	-0.01 ± 0.41 [*]	0.18 ± 0.16 [*]	0.03 ± 0.33 [†]	0.04 ± 0.03 [†]	-0.06 ± 0.23 ^S
Alvim	-0.01 ± 0.20 [*]	-0.07 ± 0.27 [*]	-0.01 ± 0.38 [*]	-0.01 ± 0.16 [*]	-0.03 ± 0.28 [†]		
Titamax EX	-0.08 ± 0.17 [*]	0.13 ± 0.48 [*]	-0.03 ± 0.28 [*]	-0.13 ± 0.18 [*]	-0.01 ± 0.34 [†]		
Sku							
Drive	3.47 ± 0.53 [*]	3.31 ± 0.73 [*]	3.31 ± 0.92 [*]	3.33 ± 0.32 [*]	3.36 ± 0.72 [†]	3.51 ± 0.27 [†]	3.18 ± 0.64 [†]
Alvim	3.66 ± 0.55 [*]	3.04 ± 0.53 [*]	3.58 ± 0.77 [*]	3.42 ± 0.28 [*]	3.43 ± 0.66 [†]		
Titamax EX	3.67 ± 0.48 [*]	3.46 ± 1.15 [*]	3.75 ± 0.58 [*]	3.50 ± 0.36 [*]	3.61 ± 0.77 [†]		
Str							
Drive	0.23 ± 0.08 ^{Aa}	0.11 ± 0.14 ^{Ba}	0.09 ± 0.02 ^{Ba}	0.19 ± 0.08 ^{Aa}	0.15 ± 0.11 [†]	0.14 ± 0.02 ^{A†}	0.07 ± 0.01 ^{BS}
Alvim	0.18 ± 0.07 ^{Ab}	0.09 ± 0.02 ^{Ba}	0.09 ± 0.03 ^{Ba}	0.18 ± 0.03 ^{Aa}	0.12 ± 0.06 [†]		
Titamax EX	0.18 ± 0.04 ^{Ab}	0.08 ± 0.01 ^{Ba}	0.14 ± 0.04 ^{Cb}	0.17 ± 0.05 ^{Aa}	0.14 ± 0.06 [†]		
Sdq							
Drive	0.40 ± 0.09 ^{Aa}	1.74 ± 0.61 ^{Ba}	1.91 ± 1.13 ^{Ba}	0.41 ± 0.05 ^{Aa}	1.26 ± 1.00 [†]	0.47 ± 0.00 ^{A†}	0.24 ± 0.02 ^{DS}
Alvim	0.45 ± 0.09 ^{Aa}	1.16 ± 0.25 ^{Bb}	0.91 ± 0.34 ^{Cb}	0.45 ± 0.06 ^{Aa}	0.80 ± 0.38 [†]		
Titamax EX	0.50 ± 0.03 ^{Aa}	1.34 ± 0.19 ^{Bb}	0.61 ± 0.08 ^{Ac}	0.48 ± 0.02 ^{Aa}	0.78 ± 0.39 [†]		
Sdr							
Drive	7.66 ± 3.07 ^{Aa}	81.86 ± 40.15 ^{Ba}	95.58 ± 73.36 ^{Ca}	7.97 ± 1.66 ^{Aa}	56.33 ± 60.86 [†]	10.08 ± 0.24 ^{A†}	2.87 ± 0.52 ^{DS}
Alvim	9.62 ± 3.49 ^{Aa}	45.84 ± 15.39 ^{Bb}	30.85 ± 17.93 ^{Cb}	9.40 ± 2.10 ^{Aa}	26.84 ± 20.11 [†]		
Titamax EX	11.15 ± 1.39 ^{Aa}	56.03 ± 11.00 ^{Bb}	15.91 ± 3.49 ^{Ac}	10.30 ± 0.79 ^{Aa}	25.96 ± 20.80 [†]		

Mean values ± standard deviations shown.

Different uppercase letters indicate significant differences in rows; different lowercase letters indicate significant differences in vertical columns; Scott-Knott and Dunnett honestly significant difference tests ($P < .05$). Different symbols represent significant differences between total results for each implant design and disks (comparison in lines and rows within the same rough parameter). *No statistically significant differences.

Factor C. For the values of Sa, shown in Table 3, there was no difference between the tops of the implants for all regions analyzed (compare $A_k B_3 \times C_n$). When the differences between the regions cervical (A_1), middle (A_2), and apical (A_3) were compared, only the implant Drive (C_2) showed differences between the regions 1, 2, and 3 in the flanks (compare $A_k B_1 \times C_2$) and the valleys (compare $A_k B_2 \times C_2$). The different portions of the threads (B_1 : flank, B_2 : valley, B_3 : top) were compared, and the valleys of the implant Drive (C_2) were always significantly rougher than the valleys in the other two

implants (C_1 and C_3) (compare $A_k B_2 \times C_n$). The flanks of the implant Drive (C_2) were also always rougher than the flanks in the other two implants (C_1 and C_3), except for the cervical region (A_1) (compare $A_k B_1 \times C_n$). Similar comparisons were done for the parameters Sdq and Sdr, as exemplified in Table 4 for Sdq. Differences between Str measurements were not significant. Therefore, the statistical analysis confirms that the design of the implant and the position in the thread (top, flank, valley) have the strongest influences on surface topography.

DISCUSSION

Modifications of implant surface topography and chemistry may alter the early bone response at different levels. By comparing micro-rough surfaces to a polished surface, Hempel et al³³ concluded that overall surface roughness, not only physicochemical properties, has a pronounced effect on osteoblast morphology, proliferation, and differentiation, although Vroom et al³⁴ found, after 12 years of follow-up, no clinical differences between turned and rough implants for either soft or hard tissue parameters.

According to Albrektsson and Wennerberg,³⁵ implants can be divided into four different categories depending on surface roughness: smooth ($Sa < 0.5 \mu\text{m}$), minimally rough (Sa between 0.5 and $1.0 \mu\text{m}$), moderately rough (Sa between 1.0 and $2.0 \mu\text{m}$), and rough ($Sa > 2.0 \mu\text{m}$). Some studies suggest that an ideal surface should show values of Sa between 1.0 and $2.0 \mu\text{m}$.³⁵⁻³⁸

In the current study, the majority of the implants presented values of Sa below $1.0 \mu\text{m}$ (minimally rough). One exception was the Drive implant, which presented Sa values in the flank and valley regions of 1.15 ± 0.45 and 1.23 ± 0.67 , respectively, but the high standard deviations indicate that there were large differences between samples.

In terms of the topography of the valleys and flanks of the threads, the dental implant macrogeometry had a strong effect on Sa . Drive and Titamax EX implants have V-threads, and Alvim implants have buttress threads. The Drive implant tended to present threads with smaller heights, whereas the Titamax EX tended to present threads with smaller external angles. Implants with V-threads present better BIC than buttress-thread implants.²⁶ The results obtained in this study might suggest that such differences could be associated with the rougher surfaces produced on the flanks and valleys of V-thread implants.

The values of Sa for the smooth disks were smaller than for all regions of all implants, confirming that the surface topography of the implants was modified in all regions by the Neoporos surface treatment.

The asymmetry of the distribution of the irregularities (Ssk) was low, independent of the macrogeometry of the implant. Since all the regions of all implants showed Ssk values close to zero, no predominance of peaks or valleys was observed in any region of any implant. A perfectly symmetric distribution of peaks and valleys would result in Ssk values equal to 0. It must be pointed out that the mean values might suggest a slight predominance of peaks in the nonthreaded region of the Drive implant ($Ssk > 0$) and a slight predominance of valleys in the nonthreaded region of the Titamax EX implant ($Ssk < 0$). However, these values can still be considered too small to represent any relevant

Table 3 Mean Values of Sq and Results of Factorial Analysis

A ₁ B _m	C _n		
	C ₁	C ₂	C ₃
A ₁ B ₁	0.9076 ^{Aa}	0.9927 ^{Ad}	0.9020 ^{Aa}
A ₁ B ₂	0.8528 ^{Ba}	2.3844 ^{Aa}	0.4269 ^{Cb}
A ₁ B ₃	0.3447 ^{Ab}	0.3296 ^{Ae}	0.3482 ^{Ab}
A ₂ B ₁	0.9143 ^{Ba}	1.4844 ^{Ac}	1.0212 ^{Ba}
A ₂ B ₂	0.5181 ^{Bb}	1.1881 ^{Ad}	0.4496 ^{Bb}
A ₂ B ₃	0.3410 ^{Ab}	0.2830 ^{Ae}	0.3614 ^{Ab}
A ₃ B ₁	0.7628 ^{Ba}	1.8711 ^{Ab}	0.9297 ^{Ba}
A ₃ B ₂	0.6848 ^{Ba}	1.1773 ^{Ad}	0.4031 ^{Bb}
A ₃ B ₃	0.3197 ^{Ab}	0.3029 ^{Ae}	0.3664 ^{Ab}

A = the region of analysis (A₁: cervical, A₂: middle, A₃: apical); B = the portion of the thread (B₁: flank, B₂: valley, B₃: top); C = the implant design (C₁: Alvim, C₂: Drive, C₃: Titamax EX).

Different lowercase letters in vertical columns indicate significant differences; different uppercase letters in horizontal rows indicate significant differences (Scott-Knott test; $P < .05$).

Table 4 Mean Values of Sdq and Results of Factorial Analysis

A ₁ B _m	C ₁	C ₂	C ₃
A ₁ B ₁	1.2076 ^{Aa}	1.3050 ^{Ad}	1.2893 ^{Aa}
A ₁ B ₂	1.0997 ^{Ba}	2.9578 ^{Aa}	0.6218 ^{Cb}
A ₁ B ₃	0.4786 ^{Ab}	0.4359 ^{Ae}	0.4887 ^{Ab}
A ₂ B ₁	1.1802 ^{Ba}	1.7523 ^{Ac}	1.4356 ^{Ba}
A ₂ B ₂	0.7272 ^{Bb}	1.3811 ^{Ad}	0.6322 ^{Bb}
A ₂ B ₃	0.4521 ^{Ab}	0.3602 ^{Ae}	0.4932 ^{Ab}
A ₃ B ₁	1.0798 ^{Ba}	2.1500 ^{Ab}	1.2880 ^{Ba}
A ₃ B ₂	0.8883 ^{Ba}	1.4049 ^{Ad}	0.5674 ^{Bb}
A ₃ B ₃	0.4331 ^{Ab}	0.3930 ^{Ae}	0.5078 ^{Ab}

A = the region of analysis (A₁: cervical, A₂: middle, A₃: apical); B = the portion of the thread (B₁: flank, B₂: valley, B₃: top); C = the implant design (C₁: Alvim, C₂: Drive, C₃: Titamax EX).

Different lowercase letters in vertical columns indicate significant differences; different uppercase letters in horizontal rows indicate significant differences (Scott-Knott test; $P < .05$).

asymmetry.²⁰ Similarly, the mean values for Sku were close to 3 in all regions of all the implants. Values of Sku close to 3, presented in conjunction with Ssk values close to 0, confirm that the topography height distribution approaches normality, independent of either the implant macrogeometry or the implant region.

An important visual feature that emerges from the 3D topographic maps shown in Figs 5 to 7 is that some regions of the examined implants presented a stronger texture. In general, the flanks showed features resembling parallel grooves oriented in one direction, the tops showed no directionality of the asperities, and the valleys showed an intermediate behavior. The

parameter *Str*, which measures the texture aspect ratio of the surfaces, is by definition between 0 and 1. Larger values, say $Str > 0.5$, indicate a uniform texture in all directions, ie, no defined lay (isotropy). Smaller values indicate an increasingly strong directional structure or lay (anisotropy).¹⁸

To summarize the results, it was verified that application of the same surface treatment to different implants nevertheless resulted in differences in their surface roughness parameters, depending particularly on the geometric design of the implant and on the region of the thread within each implant.

It is known that the blasting variables, such as blasting media size, velocity, and surface coverage, can produce different surface topography features.³⁹ In the present study, for all the implants, the flanks and valleys of the threads presented higher and steeper asperities than the tops of threads and the nonthreaded regions. This may suggest that the angles of the threads cause abrasive particles to rebound to/from flanks and valleys, increasing the severity of material displacement and/or removal from the surface. These effects were more relevant for the Drive implant, which featured threads with smaller heights, for which the interaction from the particles hitting the flanks and valleys was probably more intense.

Moreover, the flanks presented stronger textures, particularly for the implants with threads with larger internal angles (Drive and Alvim). This may suggest that, when the abrasive particles that are used to treat the surfaces impinge the flanks of the threads, the slope between the thread and the incident particles leads to their preferential attack at certain angles. Similar effects were found at the valleys of the threads with larger internal angles (Drive and Alvim), but not for the Titamax EX implant, which presents less steep threads. This suggests that the particles with a preferential attack angle at the flank of the threads still act on the valleys, mainly when the threads are steep.

The present study only characterized the surface topography of the implants using laser interferometry and SEM. Differences in surface topography were seen, depending on the region and macrogeometry of the implant. It is expected that these differences in surface topography could result in differences in cell proliferation at different regions of an implant. This is an important hypothesis to investigate and requires *in vitro* cell proliferation studies. The present study showed that flat disks subjected to the same surface treatment as dental implants do not represent the surface topography of all regions of that implant, but only the regions that have a similar angle between the surface and the abrasive particles. Therefore, *in vitro* studies might examine commercially available implants in addition to flat disks to detect possible differences.

Interestingly, a recent *in vitro* study investigated cell adhesion and proliferation directly onto titanium screws that had been coated with zirconium nitride by physical vapor deposition.⁴⁰ Although not emphasized by the authors, the results suggested that cell growth was much less intense on the tops than on the flanks and valleys of the screws.

Cell growth studies using both screws and flat disks to examine the surface treatment used in this study, as well as other surface treatments, are currently in progress.

CONCLUSIONS

The results shown in this paper provide evidence that the macrogeometry of dental implants, which consists of threaded regions with particular thread angles and heights, has a significant effect on their surface topography parameters. Therefore, knowledge of the type of surface finish applied to dental implants is not sufficient to characterize their final surface topography.

The macrogeometry of the implants did not influence parameters associated with the distribution of the heights of the irregularities (skewness and kurtosis). On the other hand, parameters associated with the height of the irregularities (arithmetical mean roughness), the slope of the asperities (root-mean-square slope), the presence of a surface texture (texture aspect ratio), and the developed surface area of the irregularities (interfacial area ratio) were significantly affected by the geometry of the implants.

Flat disks subjected to the same surface treatment applied to a dental implant do not represent the surface topography of all regions of that implant, but only those regions that have a similar angle between the surface and the abrasive particles.

ACKNOWLEDGMENTS

The authors are grateful to Neodent for providing all the samples used in this work and to Fundação de Apoio à Pesquisa no Estado de Minas Gerais (Fapemig), Brazil, and Conselho Nacional de Desenvolvimento Científico e Tecnológico (CNPq), Brazil, for financial support. The authors reported no conflicts of interest related to this study.

REFERENCES

1. Brånemark PI, Breine U, Adell R, Hansson B, Lindström J, Ohlsson A. Intra-osseous anchorage of dental prostheses: I. Experimental studies. *Scand J Plast Reconstr Surg* 1969;3:81–100.
2. Chuang SK, Cai T. Predicting clustered dental implant survival using frailty methods. *J Dent Res* 2006;85:1147–1151.

3. Levine RA, Clem D, Beagle J, Ganeles J, Johnson P, Solnit G. Multicenter retrospective analysis of the solid-screw ITI implant for posterior single-tooth replacements. *Int J Oral Maxillofac Implants* 2002;17:550–556.
4. Zupnik J, Kim SW, Ravens D, Karimbux N, Guze K. Factors associated with dental implant survival: A 4-year retrospective analysis. *J Periodontol* 2011;82:1390–1395.
5. Trisi P, Lazzara R, Rebaudi A, Rao W, Testori T, Porter SS. Bone implant contact on machined and dual acid-etched surfaces after 2 months of healing in the human maxilla. *J Periodontol* 2003;74:945–956.
6. Shibli JA, Grassi S, de Figueiredo LC, et al. Influence of implant surface topography on early osseointegration: A histological study in human jaws. *J Biomed Mater Res B Appl Biomater* 2007;80:377–385.
7. Soskolne WA, Cohen S, Sennerby L, Wennerberg A, Shapira L. The effect of titanium surface roughness on the adhesion of monocytes and their secretion of TNF-alpha and PGE2. *Clin Oral Implants Res* 2002;13:86–93.
8. Buser D, Nydegger T, Oxland T, et al. Interface shear strength of titanium implants with a sandblasted and acid-etched surface: A biomechanical study in the maxilla of miniature pigs. *J Biomed Mater Res* 1999;45:75–83.
9. Buser D, Schenk RK, Steinemann S, Fiorellini JP, Fox CH, Stich H. Influence of surface characteristics on bone integration of titanium implants. A histomorphometric study in miniature pigs. *J Biomed Mater Res* 1991;25:889–902.
10. Abbron A, Hopfensperger M, Thompson J, Cooper LF. Evaluation of a predictive model for implant surface topography effects on early osseointegration in the rat tibia model. *J Prosthet Dent* 2001;85:40–46.
11. Novaes ABJ, Souza SL, de Oliveira PT, Souza AM. Histomorphometric analysis of the bone-implant contact obtained with 4 different implant surface treatments placed side by side in the dog mandible. *Int J Oral Maxillofac Implants* 2002;17:377–383.
12. Wennerberg A, Albrektsson T. Suggested guidelines for the topographic evaluation of implant surfaces. *Int J Oral Maxillofac Implants* 2000;15:331–344.
13. Kilpadi D, Lemons J. Surface energy characterization of unalloyed titanium implants. *J Biomed Mater Res* 1994;28:1419–1425.
14. Vercaigne S, Wolke JGC, Naert I, Jansen JA. The effect of titanium plasma-sprayed implants on trabecular bone healing in the goat. *Biomaterials* 1998;19:1093–1099.
15. Bennett JM, Mattsson L. *Introduction to Surface Roughness and Scattering*. Washington DC: Optical Society of America, 1999.
16. Dong SP, Mainsah E, Sullivan PJ, Stout KJ. Instruments and measurement techniques of 3-dimensional surface topography. In: Stout KJ (ed). *Three Dimensional Surface Topography: Measurement, Interpretation and Applications*. London: Penton Press, 1994:3–63.
17. ISO 4287. *Geometrical Product Specifications (GPS) - Surface Texture: Profile Method - Terms, Definitions and Surface Texture Parameters*. Geneva: International Organization for Standardization, 1997.
18. Stout KJ, Sullivan PJ, Dong WP, et al. *The Development of Methods for the Characterization of Roughness in Three Dimensions*. University of Birmingham and L'Ecole Centrale de Lyon: Butterworth Heinemann, 1993.
19. Dong WP, Sullivan PJ, Stout KJ. Comprehensive study of parameters for characterizing 3-dimensional surface-topography. 2. Statistical properties of parameter variation. *Wear* 1993;167:9–21.
20. Dong WP, Sullivan PJ, Stout KJ. Comprehensive study of parameters for characterizing 3-dimensional surface-topography. 3. Parameters for characterizing amplitude and some functional-properties. *Wear* 1994;178:29–43.
21. Coelho PG, Granato R, Marin C, Teixeira HS. The effect of different implant macrogeometries and surface treatment in early biomechanical fixation: An experimental study in dogs. *J Mech Behav Biomed Mater* 2011;27:1974–1981.
22. Deporter D. Dental implant design and optimal treatment outcomes. *Int J Periodontics Restorative Dent* 2009;29:625–633.
23. Degidi M, Piattelli A. 7-year follow-up of 93 immediately loaded titanium dental implants. *J Oral Implantol* 2005;31:25–31.
24. Javed F, Romanos GE. The role of primary stability for successful immediate loading of dental implants. A literature review. *J Dent* 2010;38:612–620.
25. Elias CN, Rocha FA, Nascimento AL, Coelho PG. Influence of implant shape, surface morphology, surgical technique and bone quality on the primary stability of dental implants. *J Mech Behav Biomed Mater* 2012;16:169–180.
26. Cardoso MV, Vandamme K, Chaudhari A, et al. Dental implant macro-design features can impact the dynamics of osseointegration. *Clin Implant Dent Relat Res* 2013 Nov 17. [Epub ahead of print]
27. Gonçalves JL Jr, Costa HL, Pessoa RS, de Mello JDB. 3D Topographic Characterization of Dental Implants. *Proceedings of The Third International Conference on Metrology*, 21–23 Mar 2012, Annecy, France.
28. Rosa MB, Albrektsson T, Francischone CE, Filho HO, Wennerberg A. Micrometric characterization of the implant surfaces from the five largest companies in Brazil, the second largest worldwide implant market. *Int J Oral Maxillofac Implants* 2013;28:358–365.
29. Rosa MB, Albrektsson T, Francischone CE, Schwartz Filho HO, Wennerberg A. The influence of surface treatment on the implant roughness pattern. *J Appl Oral Sci* 2012;20:550–555.
30. ISO/IS 11562. *Metrological Characterization of Phase Correct Filters and Transmission Bands for Use in Contact (Stylus) Instruments*. Geneva: International Organization for Standardization, 1993.
31. Scott AJ, Knott MA. A cluster analysis method for grouping means in the analysis of variance. *Biometrics* 1974;30:507–512.
32. Dunnett CW, Tamhane AC. Comparisons between a new drug and active and placebo controls in an efficacy clinical-trial. *Stat Med* 1992;11:1057–1063.
33. Hempel U, Hefti T, Dieter P, Schlottig F. Response of human bone marrow stromal cells, MG-63, and SaOS-2 to titanium based dental implant surfaces with different topography and surface energy. *Clin Oral Implants Res* 2013;24:174–182.
34. Vroom MG, Sips P, de Lange GL, et al. Effect of surface topography of screw-shaped titanium implants in humans on clinical and radiographic parameters: A 12-year prospective study. *Clin Oral Implants Res* 2009;20:1231–1239.
35. Albrektsson T, Wennerberg A. Oral implant surfaces: Part 1—Review focusing on topographic and chemical properties of different surfaces and in vivo responses to them. *Int J Prosthodont* 2004;17:536–543.
36. Wennerberg A, Albrektsson T. Effects of titanium surface topography on bone integration: A systematic review. *Clin Oral Implants Res* 2009;20(suppl 4):172–184.
37. Wennerberg A, Albrektsson T. On implant surfaces: A review of current knowledge and opinions. *Int J Oral Maxillofac Implants* 2010;25:63–74.
38. Elias CN, Meirelles L. Improving osseointegration of dental implants. *Expert Rev Med Devices* 2010;7:241–256.
39. Valverde GB, Jimbo R, Teixeira HS, Bonfante EA, Janal MN, Coelho PG. Evaluation of surface roughness as a function of multiple blasting processing variables. *Clin Oral Implants Res* 2013;24:238–242.
40. Rizzi M, Gatti G, Migliario M, Marchese L, Rocchetti V, Renò F. Effect of zirconium nitride physical vapor deposition coating on preosteoblast cell adhesion and proliferation onto titanium screws. *J Prosthetic Dent* 2014;112:1103–1110.

Copyright of International Journal of Oral & Maxillofacial Implants is the property of Quintessence Publishing Company Inc. and its content may not be copied or emailed to multiple sites or posted to a listserv without the copyright holder's express written permission. However, users may print, download, or email articles for individual use.

CAPÍTULO 2

EFFECT OF SURGICAL PLACEMENT ON THE SURFACE TOPOGRAPHY OF DENTAL IMPLANTS OF DIFERENT MACROGEOMETRY

Marina Melo Naves, Helder Henrique Machado Menezes, Denildo Magalhães,
Jessica Afonso Ferreira, José Daniel Biasoli de Mello, Henara Lillian Costa.

The International Journal of Oral and Maxillofacial Implants

EFFECT OF SURGICAL PLACEMENT ON THE SURFACE TOPOGRAPHY
OF DENTAL IMPLANTS OF DIFERENT MACROGEOMETRY

Marina Melo Naves* ^{1,2}, PhD.

Helder Henrique Machado Menezes ², M. Sc., Lecturer.

Denildo Magalhães^{1,2}, PhD, Professor.

Jessica Afonso Ferreira¹, M. Sc. Student.

José Daniel Biasoli de Mello³, Dr. Ing., Professor.

Henara Lillian Costa ³, PhD, Associate professor.

¹ School of Dentistry, Universidade Federal de Uberlândia, Campus Umuarama, Av. Pará, 1720 Bl. 4L 38.401-136, Uberlândia, Brazil.

² HD Ensinos Odontológicos, Rua Guaicurús 157 – Saraiva 38408-394, Uberlândia Brazil.

³ Laboratory of Tribology and Materials, Universidade Federal de Uberlândia, Campus Sta. Monica, Bl. 5K 38400-901, Uberlândia, Brazil.

***Corresponding author:** Marina Melo Naves. School of Dentistry, Universidade Federal de Uberlândia, Periodontology Department, Campus Umuarama, Av. Pará, 1720 Bl. 4L 38.401-136, Uberlândia, Brazil. Email: melo.naves@gmail.com

ABSTRACT

Purpose: Surface treatment alone may not determine the final microtopography of a dental implant, which can be influenced by the implant design and implant insertion procedure into bone. This work analyzed the effects of implant insertion into bone on surface roughness parameters for the same treatment applied by the same manufacturer for implants with differing macro-designs.

Materials and Methods: Three groups of titanium implants with different macro-designs were investigated using laser interferometry and scanning electron microscopy. Relevant surface roughness parameters were calculated for different regions of each implant before (B) and after (A) insertion into pork ribs.

Results: The tops of the threads of all B implants had very similar roughness parameters, independent of the geometry of the implant, and after bone insertion, this was the region that presented significant alterations. In contrast, the flanks and valleys of the threads presented higher irregularities (*Sa*) with greater slopes (*Sdq*) than the tops on all B implants, particularly for implants containing threads with smaller heights. The flanks and valleys displayed stronger textures (*Str*) than the tops, particularly on the implants with threads with larger internal angles.

Conclusions: This preliminary study demonstrated surface damage of the implants after implant installation process by the changes observed on roughness parameters, affected by the macrogeometry.

Key words: dental implants, implant design, osseointegration, surface texturing, surface topography, titanium

1. Introduction

The rehabilitation of the odontostomatognathic system by surgical and prosthetic techniques is frequently allowed by dental implants. The long-term success of the implant is determined by several factors (1-3) among which osseointegration (4-6) plays a dominant role as pointed out early in the 1970s by Brånemark (7-9). In addition to biocompatible chemistry of the material, the surface morphology of the implant is important for both primary stability and long-term bone integration (10-15). Research and development in the field of implant dentistry are frequently focused on implant redesign (eg, topography, implant surface, macro-design) to continue improving implant success rates. Newer implant designs seek to address situations that are prone to failure, such as jawbone with low density or patients with systemic diseases that compromise healing, and to reduce bone trauma and prosthetic fractures especially when an immediate load is applied. Emerging new developments are based, for example, on modification of either the chemical or the mechanical properties of an implant. They are expected to improve the host tissue response and to accelerate the healing process, allowing the best coupling to bone tissue. (4,16).

The amount of bone-to-implant contact (BIC) is an important determinant in the long-term success of dental implants. Consequently, maximization of BIC and osseointegration has become a goal of treatment, which apparently can be enhanced by varying the roughness of the implant surface (17). Evaluations have demonstrated that implants with rough surfaces show better bone apposition and BIC than implants with smooth surfaces (18, 19). Surface

roughness also has a positive influence on cell migration and proliferation, which in turn leads to better BIC, suggesting that the microtopography of titanium implants influences the biomaterial-tissue interaction (20, 21). Precise quantification of an implant's surface roughness is necessary to analyze the effects of its microtopography on such outcomes as BIC and osseointegration.

A quantitative evaluation of surface topography can be carried out using instruments with mechanical contact methods (profilometry, atomic force microscopy) or optical instruments (optical interferometry) (22). Screw-type implants contain threads with deep valleys, which makes evaluation by optical interferometry better (23, 24). After the implant's surface is assessed, different parameters (two-dimensional - 2D roughness parameters and three-dimensional - 3D roughness parameters) can be calculated to quantify its topography (25-27).

For dental implants, several parameters should be evaluated: three height parameters (arithmetic mean roughness [Sa], peakedness of the topography height distribution, also known as kurtosis [Sku], and skewness of topography height distribution [Ssk]); one spatial parameter (texture aspect ratio of the surface [Str]); and one hybrid parameter (root-mean-square slope of the surface [Sdq]).

Changes in implant macrogeometry have also contributed to implant success, directly affecting primary stability (28-30). Results in the literature (31) suggest that the insertion torque of conical implants is higher than that of cylindrical implants. This behavior can be attributed to differences in thread shape, implant geometry, and surface area. The thread geometry of conical

implants means that a larger surface area is in contact with the host tissue (32). Thus, the best dental implant design may be chosen for its placement in critical sites to improve primary stability. Dental implant macro-design features, particularly thread pattern and thread pitch, can be responsible for differences in the amount of bone surrounding the implant and in the degree of bone apposition, and they may impact the success of the establishment and/or maintenance of implant osseointegration (33).

It has been shown that surface roughness can vary according to its location on the implant, and the flat disks do not represent the implant surface (34). Therefore, in screw-type implants it is necessary to measure surface topography in three regions of the threads: flank, top, and bottom (22, 35, 36). Although this characterization is well defined, it is unclear whether the increasingly complex surface features found on modern dental implants are retained after bone insertion.

During placement of osseointegrated implants, the insertion torque may result in varied levels of compressive stresses transmitted to the adjacent bone, given that the implant bed is slightly narrower than the diameter of the implant to be placed in order to optimize primary stabilization (37, 38). Clinical studies have demonstrated a close relationship between initial stabilization and the success of an osseointegrated implant (39-41), which can be measured by the insertion torque during implant placement (40). The insertion torque must exceed 30 N.cm to obtain predictable success rates (40), aiming to avoid implant micromovement and consequent connective tissue formation (41). However, an excessively high insertion torque, above 50 N.cm (42), can occur

during dense bone implant placement (40, 43), resulting in the transmission of high compressive stresses to the adjacent bone, in addition to compromising osseointegration success (44).

The understanding of the effect of insertion torque that can be used during implant placement, without causing excessive stress in the bone tissue, is decisive for the success of implant osseointegration, since this procedure do not change topography. A few studies (45-47) demonstrated that shearing forces during the insertion procedure alters the surface of dental implants.

However, considering the lack of studies associating surface characteristics to its maintenance during implant placement and the unclear methodology to analyze this procedure related to implant design, this paper analyzes the hypothesis that a certain type of surface modification, when applied to implants with different macrogeometries, can result in different surface roughness parameters, and the effect of insertion torque used during implant placement can change topography.

Therefore, the aim of this study was to characterize the surface topography of three commercially available titanium implants with different macrogeometries, produced by the same manufacturer, which had their surface modified by a process that includes sandblasting and acid etching. In addition, it was evaluated the influence of implant placement on surface topography in cortical and cancellous bones on its surface topography was evaluated. The applicability of the methodology for morphological characterization of implants before and after implantation was also tested.

2. Materials and methods

2.1. Description of the Samples

This study investigated three groups (Drive, Alvim, and Titamax EX) of bone-compacting, commercially pure (grade 4) titanium implants produced by the same company (Neodent). Compacting-type implants were chosen because they present a conical or hybrid design, where the apical region is narrower than the cervical region. All implants featured a Morse taper connection and had a diameter of 3.5 mm and a length of 13 mm. However, they presented with different macrogeometries, as shown in Fig 1 (34). Three samples of each implant type were assessed before (B) and other three samples were assessed after (A) implant placement in pork ribs.

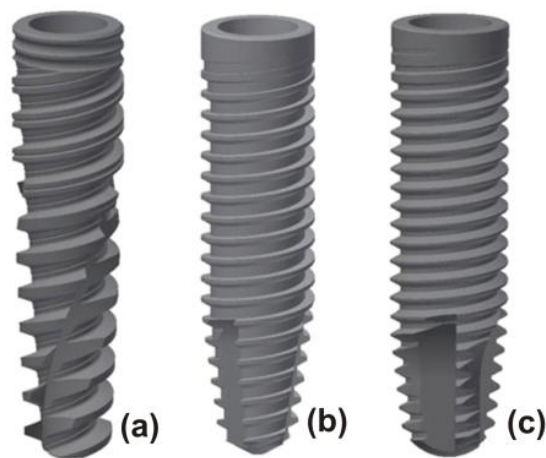


Figure 1. Implant macrogeometries. (a) Drive; (b) Alvim; (c) Titamax EX.

The surface modification applied to all implants was identical and was a trademark of the company (Neoporos, Neodent). The surface modification method, sand blasted acid etching (SBAE) consists of, first, blasting using abrasive particles with automated control of the velocity, direction, pressure,

and size of particles. In sequence, the aluminum oxide particles of controlled size create craters on the surface of the implant. Finally, acid etching is used to ensure uniform surface topography.

2.2. Implant placement into pork ribs

Fresh pork ribs were prepared and used as experimental model. Three implants of each design (n=9) was inserted into fresh porcine ribs (D3 quality) (48), with 15 mm height and 150 mm length. Considering that the pigs were not sacrificed for research matters, this study did not have the necessity of ethical animal committee approval (49, 50). The ribs were fixed on a clamp with manual adjustment. The insertion of the dental implants were made according to manufacturer instructions, up to 13mm depth (Fig. 2A, 2B). The distance between each implant was 20 mm. The implant fixture was inserted using a dynamometric driver set to maximum 60 Ncm torque. Computed tomography (CT) was used to verify the exact position of each screw (Fig. 2C, 2D, 2E, 2F, 2G). After insertion, the implant was removed using lateral cutting of bone with piezoelectric instrument, taking care not to affect the sample surfaces, i.e. the removal procedure did not damage the implant surface.

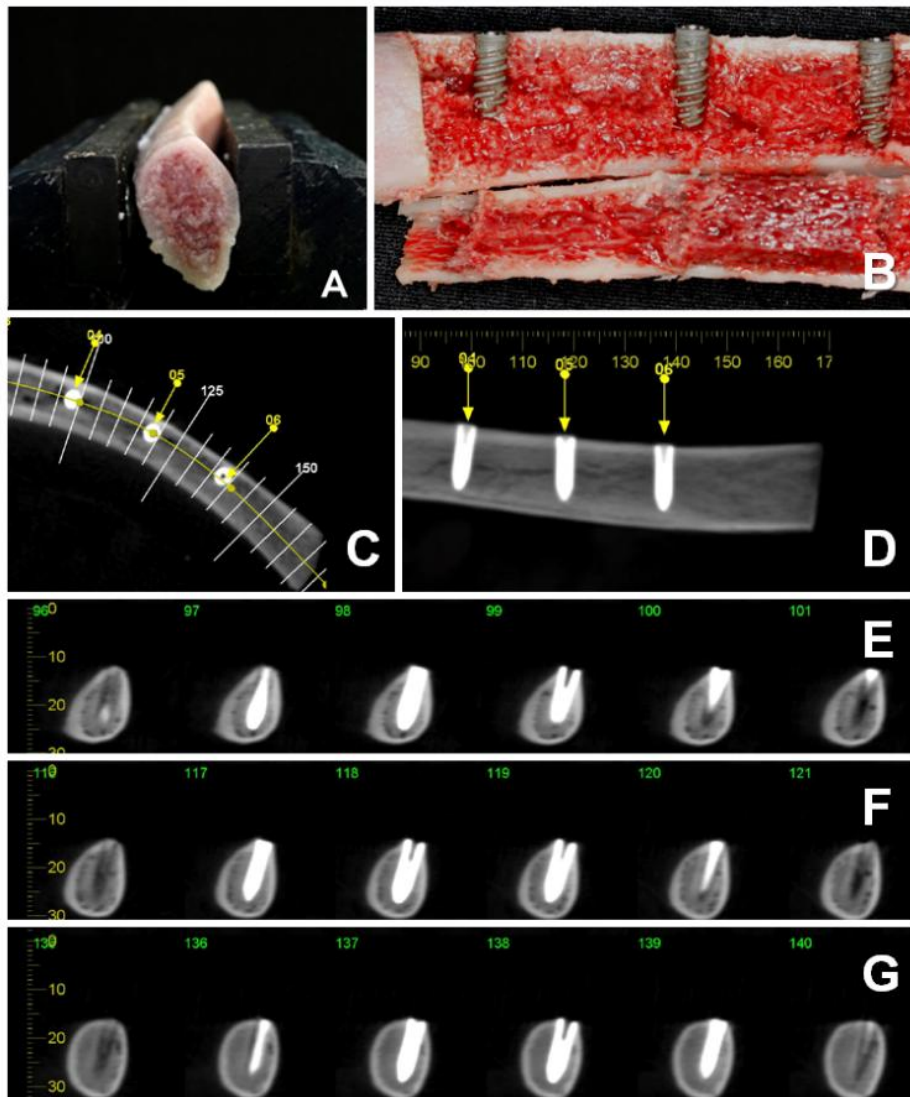


Figure 2. (a) Pork rib. (b) Pork rib of Drive implants sectioned. (c, d) transversal CT of Titamax EX implants. (e, f, g) axial CT of pork rib with Titamax EX implants.

The implants were cleaned from osseous matter by submerging them into a glass tube in purified water (30 minutes) and acetone (10 minutes) to remove residual bone debris from the surface, as suggested by Senna et al. (47). Acetone is an organic solvent known to be nonreactive to titanium and ceramics and commonly used to remove contaminants from titanium implants.

2.3. Surface Characterization

Laser interferometry and scanning electron microscopy (SEM) were used for surface characterization of the implants. A 3D laser interferometer (UBM MESSTECHNIK MicroFocus) was used to assess the surface topography of the dental implants. Measurement densities of $1,000 \times 1,000$ points were used. The measuring rate was 300 points/s and continuous measurement mode was used. The measurement area (0.8×0.4 mm) was chosen so that it could include at least one thread for all the regions without losing focus (34).

Because the implants featured complex macrogeometry, different areas were measured for each implant, as exemplified in Fig 3. There were 18 samples: six Drive implants, six Alvim implants, six Titamax EX implants, all finished by sand blasting acid etching (SBAE). Each implant was divided into three regions (cervical [1], middle body [2], and apical [3]) (Fig 3a). Then, for each region (cervical, middle body, and apical), three consecutive thread tops, three consecutive thread valleys, and three consecutive thread flanks were measured separately (Fig 3b) with dimensions (0.8×0.4 mm), for a total of 27 measurements per implant.

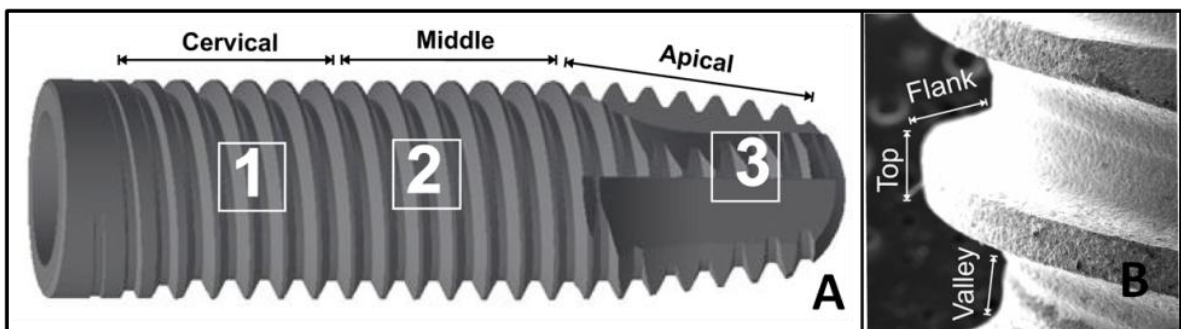


Figure 3. (a) Regions of analysis of the implants. (b) Analysed areas of regions 1, 2 and 3.

Surface topography characterization consists of three components: form, waviness, and roughness. For topographic evaluation, it is necessary to separate these components using filters. After form removal, a filtering process separated waviness and surface roughness. It used a $50 \times 50\mu\text{m}$ Gaussian filter, according to ISO 11562 (51) recommendations. To characterize the macrogeometry of the implants, profiles of the threads were selected after form removal (Fig 4). MountainsMap software (Digital Surf) was used for this purpose, and it also provided visual 2D and 3D images of the surfaces and numeric descriptions of their surface roughness parameters. Vertical heights (Fig 4a) and angles (Fig 4b) of the threads were measured to quantify the macrogeometry of the each implant (34). When the geometry of the thread was complex, the software MB Ruler (Markus Bader MB-Software solutions, Iffezheim, Germany) was used to calculate the angles (Fig 4c).

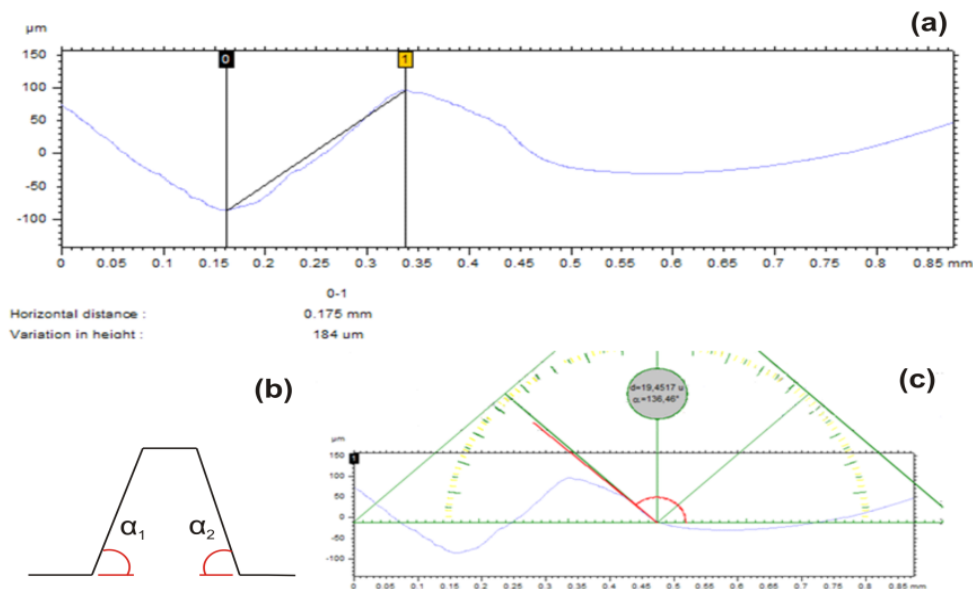


Figure 4. Parameters measured to characterize the macrogeometry of the implants. (a) Thread height. (b) Thread angles. (c) Scheme for angle measurement in threads with complex shape (34)

The numeric description of the surface roughness of the implants in the different regions of the threads used the following roughness parameters: S_a , S_{sk} , S_{ku} , S_{tr} and S_{dq} , as suggested by Wennerberg and Albrektsson (22). Mathematic descriptions of those parameters can be found in Stout et al. (25). SEM imaging of the tops, flanks, and valleys of the threads, was carried out before and after implantation to provide a qualitative analysis of the surfaces (EVO MA 10, Carl Zeiss) under different magnifications and an acceleration voltage of 15 kV. This surface characterization was conducted in three implants of each macrogeometry before the placement into pork ribs (B implants) and three implants of each macrogeometry after placement into pork ribs (A implants).

2.4. Statistical analysis

For each parameter, mean and SD were calculated for each implant before and after implant insertion. To evaluate the statistical significance, the roughness parameters data before and after implant insertion were analyzed by paired t-test ($\alpha = 0.05$) (SPSS Statistics Base 17.0 – IBM, Chicago, USA).

3. Results

Implant insertion torque never exceeded the maximum value recommended by the manufacturer. Average insertion torque (Ncm) of 60 ± 0 , 60 ± 0 , and 50 ± 8.6 was calculated for Drive, Alvim, and Titamax EX implants, respectively.

Table 1 presents the values for the parameters used to characterize the threads in the three different regions of each B implant (34). Some variation in the angles and heights between the different regions of the same implant was apparent. The Drive implant tended to present threads with smaller heights, whereas the implant Titamax EX tended to present threads with smaller external angles.

Table 1: Macrogeometrical measurements of the implants, where α_1 and α_2 are the internal angles of the threads and h is the height of the fillets.

Implant	Region	α_1 (degrees)	α_2 (degrees)	Height, h (μm)
Drive	Region 1	45.0	66.0	104
	Region 2	46.3	38.5	149
	Region 3	52.3	43.5	157
	Mean	48.6		137
Alvim	Region 1	37.3	27.2	223
	Region 2	43.9	43.5	184
	Region 3	59.4	37.1	138
	Mean	41.4		182
Titamax EX	Region 1	18.8	17.4	212
	Region 2	35.8	33.2	238
	Region 3	29.0	43.6	162
	Mean	29.6		204

The top two rows of Fig 5 shows global images of all the implants before osseous insertion (B) at low magnifications (Fig. 5A, 5B, 5C) (34)., and after bone insertion (A) (Fig 5d, 5e, 5f). Although images are very similar for both conditions, it is possible to observe regions of a small surface deformation (arrow, f) and contamination (arrow, d) on SEM of A implants. When the tops of the threads were viewed under high magnification, the morphology of all B implants appeared very similar (Fig. 5g, 5h, 5i) (34). For all A implants, it is

possible to observe minor changes, suggesting a small plastic deformation of the surface irregularities for the three different implants (Fig. 5j, 5k, 5l).

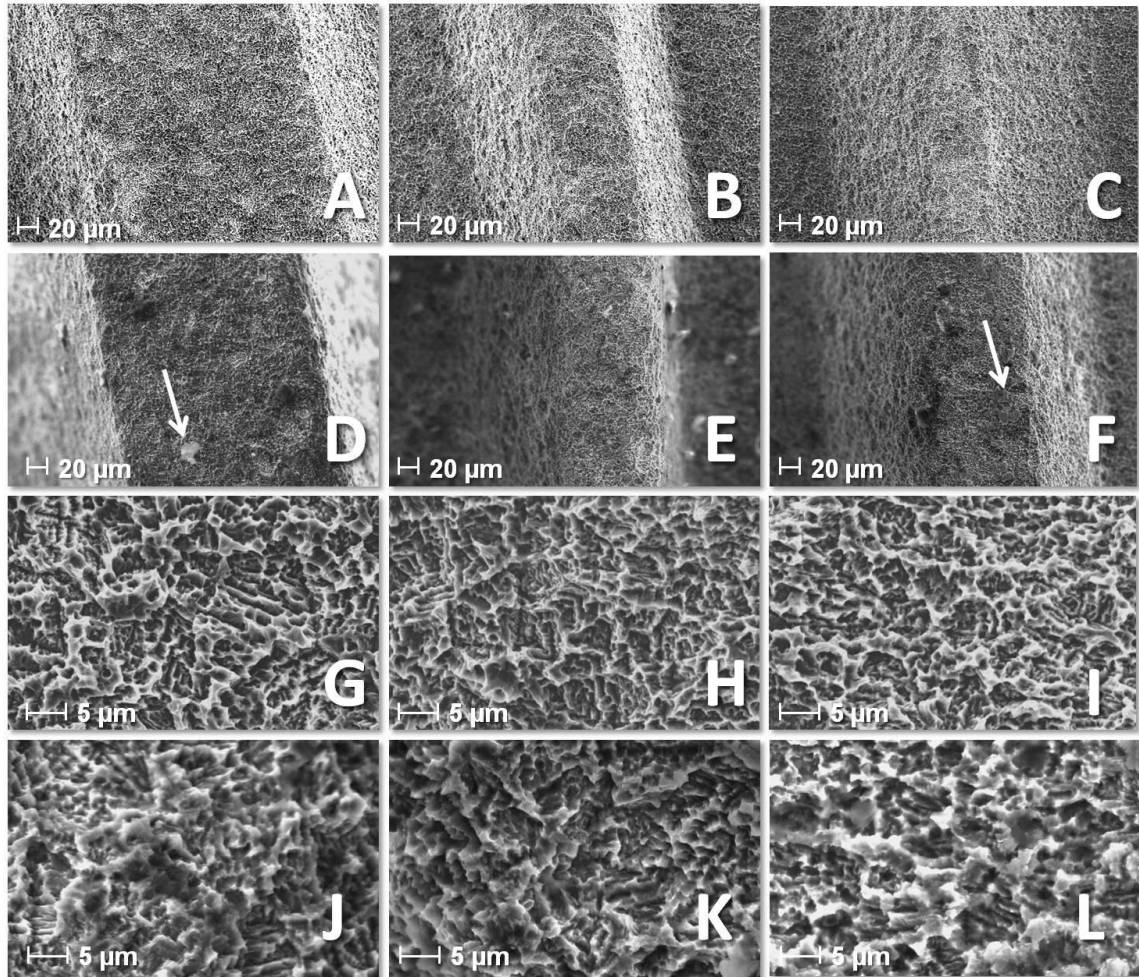


Figure 5. SEM of the implants: (A) Drive B, top, (B) Alvim B, top, (C) Titamax EX B, top; (D) Drive A, top, (E) Alvim A, top, (F) Titamax EX A, top; (G) zoom showing a typical top of Drive B, (H) top of Alvim B, (I) top of Titamax EX B, (J) zoom showing a typical top of Drive A, (K) top of Alvim A, (L) top of Titamax EX A .

The mean values \pm standard deviations of the surface roughness parameters (*Sa*, *Ssk*, *Sku*, *Str*, and *Sdq*) were averaged along regions 1, 2, and 3 of each type of dental implant (B and A) and are shown in Table 2. For the valleys and flanks of the threads the dental implant macrogeometry had a strong effect on *Sa*. Values for *Sa* of flank and valley for Drive and Alvim implants had a significant reduction after bone insertion (flank: Drive $p=.005$ / Alvim $p=.045$ and valley: Drive $p=.000$ / Alvim $p=.022$). For Titamax EX implant, these values of *Sa* for tops and flanks had increased, but not statistically significant. For the top, *Sa* increased after osseous insertion for all implants, mainly on Alvim ($p=.0009$). As the standard deviation was high, the top of the threads may present irregular surface on A implants.

The parameters associated with the distribution of the heights of the surface irregularities are *Ssk* and *Sku*. All the regions of all B and A implants showed *Ssk* values close to 0 and values of *Sku* close to 3 (Fig. 6). *Ssk* values of top for the Drive implant became negative, indicating discrete deformation of roughness peaks ($p<.04$) (Tab. 2). Other implant design and areas did not have *Ssk* values significantly changed.

Table 2: Surface roughness parameters measured at four different sites on commercial screw-type implants before – B (34) and after – A osseous insertion using laser interferometry – mean values \pm standard deviation (SD) (* $p < .05$ between before and after bone insertion implants)

Implant	Before/After	Top	Flank	Valley	total
Sa (SD) μm					
Drive	B	0.24 \pm 0.04	1.15 \pm 0.45	1.23 \pm 0.67	0.81 \pm 0.64
	A	0.37 \pm 0.41	0.71 \pm 0.57*	0.43 \pm 0.36*	0.51 \pm 0.41*
Alvim	B	0.26 \pm 0.04	0.69 \pm 0.13	0.54 \pm 0.21	0.47 \pm 0.23
	A	0.63 \pm 0.66*	0.58 \pm 0.22*	0.42 \pm 0.19*	0.51 \pm 0.41
Titamax EX	B	0.28 \pm 0.02	0.73 \pm 0.14	0.33 \pm 0.04	0.43 \pm 0.21
	A	0.33 \pm 0.27	0.87 \pm 0.58	0.45 \pm 0.71	0.52 \pm 0.57
Ssk (SD)					
Drive	B	0.06 \pm 0.16	-0.01 \pm 0.40	-0.01 \pm 0.41	0.03 \pm 0.33
	A	0.07 \pm 0.24*	0.14 \pm 0.59	-0.07 \pm 0.25	0.00 \pm 0.38
Alvim	B	-0.01 \pm 0.20	-0.07 \pm 0.27	-0.01 \pm 0.38	-0.03 \pm 0.28
	A	0.16 \pm 0.59	-0.12 \pm 0.44	0.08 \pm 0.59	0.04 \pm 0.54
Titamax EX	B	-0.08 \pm 0.17	0.13 \pm 0.48	-0.03 \pm 0.28	-0.01 \pm 0.34
	A	-0.20 \pm 0.53	0.16 \pm 0.41	-0.12 \pm 0.20	-0.05 \pm 0.40
Sku (SD)					
Drive	B	3.47 \pm 0.53	3.31 \pm 0.73	3.31 \pm 0.92	3.36 \pm 0.72
	A	4.07 \pm 1.67	3.72 \pm 1.64	3.20 \pm 0.61	3.64 \pm 1.36
Alvim	B	3.66 \pm 0.55	3.04 \pm 0.53	3.58 \pm 0.77	3.43 \pm 0.66
	A	4.83 \pm 3.93	3.81 \pm 1.97	4.40 \pm 4.04	4.24 \pm 3.27
Titamax EX	B	3.67 \pm 0.48	3.46 \pm 1.15	3.75 \pm 0.58	3.61 \pm 0.77
	A	5.01 \pm 3.41	3.58 \pm 1.47	3.52 \pm 0.58	3.99 \pm 2.15
Str (SD) μm					
Drive	B	0.23 \pm 0.08	0.11 \pm 0.14	0.09 \pm 0.02	0.15 \pm 0.11
	A	0.18 \pm 0.10*	0.15 \pm 0.25	0.12 \pm 0.09	0.15 \pm 0.16
Alvim	B	0.18 \pm 0.07	0.09 \pm 0.02	0.09 \pm 0.03	0.12 \pm 0.06
	A	0.11 \pm 0.07*	0.04 \pm 0.03*	0.09 \pm 0.09	0.09 \pm 0.08*
Titamax EX	B	0.18 \pm 0.04	0.08 \pm 0.01	0.14 \pm 0.04	0.14 \pm 0.06
	A	0.21 \pm 0.12	0.03 \pm 0.02*	0.23 \pm 0.17*	0.16 \pm 0.14
Sdq (SD) μm					
Drive	B	0.40 \pm 0.09	1.74 \pm 0.61	1.91 \pm 1.13	1.26 \pm 1.00
	A	0.62 \pm 0.68	1.03 \pm 0.69*	0.69 \pm 0.57*	0.74 \pm 0.64*
Alvim	B	0.45 \pm 0.09	1.16 \pm 0.25	0.91 \pm 0.34	0.80 \pm 0.38
	A	0.82 \pm 0.64*	0.89 \pm 0.36*	0.67 \pm 0.31	0.74 \pm 0.47
Titamax EX	B	0.50 \pm 0.03	1.34 \pm 0.19	0.61 \pm 0.08	0.78 \pm 0.39
	A	0.53 \pm 0.33	1.49 \pm 1.34	0.72 \pm 1.09	0.86 \pm 1.05

Although *Sku* values for top and flank had increased for all implants after bone insertion, this aspect is not significant when we consider the physical meaning of statistical numerical values as a general observation, all implants had their *Sku* values higher after bone insertion, indicating discrete deformation of the surface peaks (Fig. 6) Also, no significant difference between values of *Sku* was found before and after bone insertion for different implants and different regions from the statistical analysis.

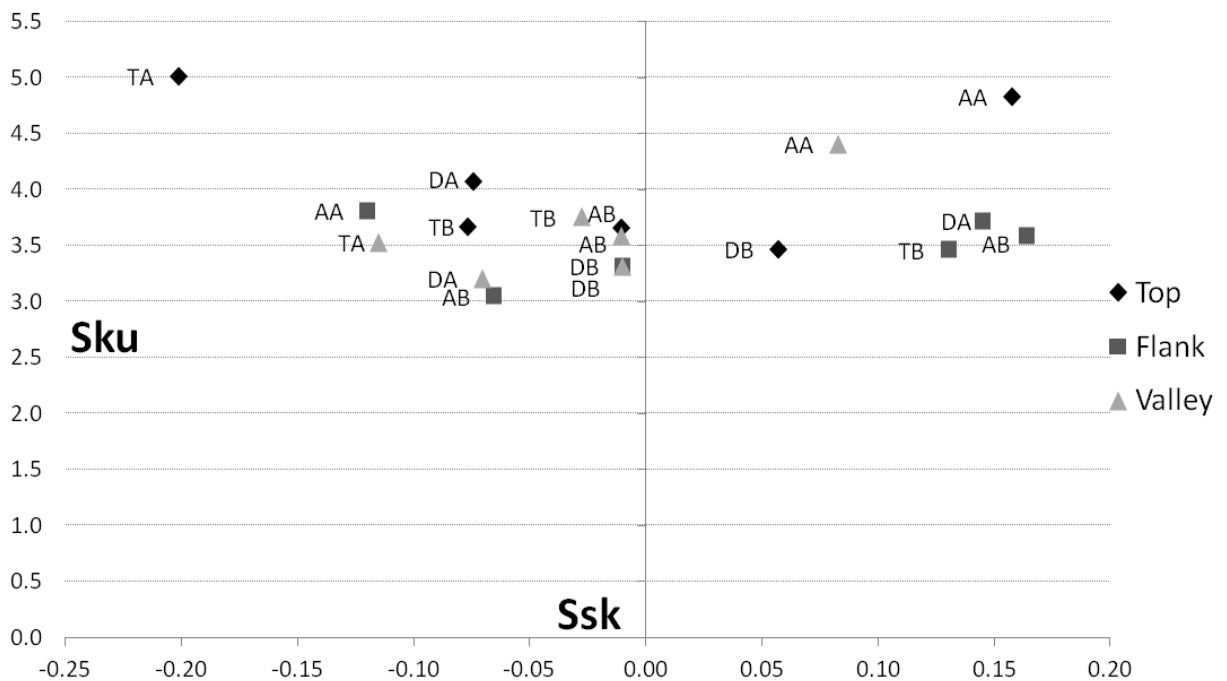


Figure 6. *Ssk* (*x*) x *Sku* (*y*) parameter for B and A implants (DB – Drive Before; DA – Drive After; AB – Alvim Before; AA – Alvim After; TB – Titamax Before; TA – Titamax After)

To quantify texture strength, ie, the uniformity of the texture, the parameter *Str*, which assesses the texture aspect ratio of the surfaces, was measured, and the results for B and A implants are shown in Table 2. All

implants showed smaller values for *Str* in the flanks and valleys of the threads than the tops, which suggests a stronger directionality on B implants (34). After osseous insertion, all implants kept their general characteristics of anisotropic surface for all regions. The top of Drive and Alvim implants increased their directionality after bone insertion ($p<.049$ and $p<.008$, respectively). The flank of Alvim and Titamax EX had a decrease of *Str* values after bone insertion, indicating an increase of directionality statistically different ($p<.000$) when compared to the same situation before bone insertion.

The values of *Sdq*, which represent the root-meansquare values of the slopes of the asperities, are also shown in Table 2. The tops of the threads showed similarities in this parameter for B implants, independent of the macrogeometry (34). After osseous insertion, A implants presented higher values of *Sdq* on the tops of all macrogeometries, but only on Alvim implant all regions were statistically different after bone insertion. The flanks and valleys of the threads showed asperities that are more inclined. The largest and most scattered values for *Sdq* were found for the flanks and valleys of the Drive B implant (34), and after osseous insertion the flank and valley of Drive implant had a strong and significant reduction ($p<.001$ and $p<.000$, respectively). Titamax EX had no statistical significant difference on *Sdq* values when comparing surface before and after bone insertion.

The results shown in Table 2 show the average results of the surface roughness parameters before (B) and after (A) osseous insertion for regions 1, 2, and 3 distinguished according to macrogeometry (Alvim B, Drive B, Titamax EX B) and the portion of the thread (top, flank, or valley). The statistical

analysis is also showed on table 2 and confirms that the design of the implant and the position in the thread (top, flank, valley) have the strongest influences on surface topography.

4. Discussion

Concerning the measurement methods, previous studies addressing surface damage also used scanning electron microscopy and interferometry (45-47). As optical interferometry is suggested to better quantify surface topography of screw type implants (22-24), we analyzed the same parameters (2D and 3D roughness parameters) before and after the implants were inserted into pork ribs. In order to provide a significant picture of the implant surfaces, SEM was also conducted in this study. To remove contaminants of implant surface after bone insertion, we followed the protocol suggested by Salerno et al. (46), and most bone residuals were removed. Observing the CT images, it was possible to evaluate the characteristic of pork ribs, presenting similarity of cortical and cancellous dimensions when compared to human jaw.

According to Albrektsson and Wennerberg (52), implants can be divided into four different categories depending on surface roughness: smooth ($Sa < 0.5 \mu\text{m}$), minimally rough (Sa between 0.5 and 1.0 μm), moderately rough (Sa between 1.0 and 2.0 μm), and rough ($Sa > 2.0 \mu\text{m}$). Some studies suggest that an ideal surface should show values of Sa between 1.0 and 2.0 μm (13, 52, 53). In the current study, which is based on results of Naves et al (34), the majority of the implants before osseous insertion (B) presented values of Sa below 1.0

μm (minimally rough). One exception was the Drive implant (B), which presented S_a values in the flank and valley regions of 1.15 ± 0.45 and 1.23 ± 0.67 , respectively, but the high standard deviations indicate that there were large differences between samples. Before implantation, the dental implant macrogeometry had a strong effect on S_a . Drive and Titamax EX implants have V-threads and Alvim implants have buttress threads. The Drive implant tended to present threads with smaller heights, whereas the Titamax EX tended to present threads with smaller external angles (34). Implants with V-threads present better BIC than buttresstthread implants (33). The results obtained in the previous study (34) might suggest that such differences could be associated with the rougher surfaces produced on the flanks and valleys of V-thread implants. Also, the insertion process may damage mainly the top of the threads with increase of S_a values. After osseous insertion, the Drive implant was the only macrogeometry that presented a strong reduction of S_a values on flank and valley, which may be attributed to the small height of the thread.

The asymmetry of the distribution of the irregularities (S_{sk}) was low, independent of the macrogeometry of the implant. Since all the regions of all implants showed S_{sk} values close to zero, no predominance of peaks or valleys was observed in any region of any implant before or after bone insertion. The top of Drive implant was the main area where deformation of the irregularities occurred, because there was predominance of peaks before bone insertion, and after this processes the top presented negative S_{sk} values, indicating predominance of valleys. This may be explained by the morphology of the top of the thread of Drive implant, presenting the largest top area between all samples

of this study. However, these values can still be considered too small to represent any relevant asymmetry (27).

Similarly, the mean values for *Sku* were close to 3 in all regions of all the implants. There were a small increase of these values on the top and flank of all implants after bone insertion independent of the macrogeometry. Although values of *Sku* were not statistically different before and after bone insertion, the increasing of these values for the top and flank of the A implants may be explained by deformation of the higher asperities during insertion process (45, 47). Values of *Sku* close to 3, presented in conjunction with *Ssk* values close to 0, confirm that the topography height distribution approaches normality, independent of either the implant macrogeometry or the implant region. As this two parameters can vary strongly with of small variations on topography, such as contaminants, it is prudent to evaluate morphological space instead the numbers on their own (54)

The parameter *Str*, which measures the texture aspect ratio of the surfaces, is by definition between 0 and 1. Larger values, say $Str > 0.5$, indicate a uniform texture in all directions, ie, no defined lay (isotropy). Smaller values indicate an increasingly strong directional structure or lay (anisotropy) (25). To summarize the results, it was verified that application of the same surface treatment to different implants nevertheless resulted in differences in their surface roughness parameters due to blasting variables (55), depending particularly on the geometric design of the implant and on the region of the thread within each implant (34). The flanks and valleys of the threads presented higher and steeper asperities than the tops of threads for all implants before

osseous insertion. After bone insertion, the top of the threads presented more alterations on asperities than other areas of the threads, specially for Drive and Alvim implants. This is expected because the top is the portion of the thread that has major contact with bone tissue during insertion in one direction, increasing directionality. On a general basis, B and A implants had their anisotropic characteristics kept. In addition, as this study did not applied removal torque on the implants as suggested by Mint et al. (45) and Senna et al. (47), the results are more trustful when compared to the study of Salerno et al. (46), where values of topography deformation showed no major changes in the apex surface micro-structure, probably due to this reverse process.

The only implant that had an increase in Sdq values on flank and valley was Titamax EX. This may be explained due to the smaller insertion torque of these implants.

The present study only characterized the surface topography of the implants using laser interferometry and SEM, before and after bone insertion. Differences in surface topography were seen, depending on the area and macrogeometry of the implant. It is expected that these differences after bone insertion in surface topography could result in differences in cell proliferation. This is an important hypothesis to investigate and requires in vitro cell proliferation studies. The present study showed that, after the implant insertion process, surface topography may change, mainly on the top of all implants. In general, the implant with smaller height of threads presented a reduction of roughness (Sa). The implant with the largest heights and smaller internal angles of the threads showed less alterations when compared to other

macrogeometries. Cell growth studies using both pre and post-insertion screws to examine the surface treatment used in this study, as well as other surface treatments are currently in progress. Within the limitations of this in vitro study, we conclude that the procedure set is appropriate for quantitative evaluation of the surface of different dental implants.

5. Conclusions

The results shown in this paper provide evidence that the macrogeometry of dental implants, which consists of threaded regions with particular thread angles and heights, has a significant effect on their surface topography parameters, except on parameters associated with the distribution of the heights of the irregularities. In addition, the insertion into bone changes topography parameters, especially on implants with larger internal angles of the threads and larger area of the tops. A small alteration for most parameters (*Sa*, *Str*, *Sdq*) was observed after bone insertion, except for *Ssk* and *Sku*.

It can be concluded that the methodology used on this study is adequate to verify surface alterations on implant placement process. Within the limitations of this in vitro study, we conclude that the procedure set is appropriate for quantitative evaluation of the surface of different implants designs and surface roughness may lightly change after implant placement.

Acknowledgments

The authors are grateful to Neodent for providing all the samples used in this work and to Fapemig (Supporting Foundation to Minas Gerais Research), CAPES, (Brazil, and CNPq (National Counsel of Technological and Scientific Development) Brazil, for financial support. The authors reported no conflicts of interest related to this study.

6. References

1. Papaspyridakos P, Chen CJ, Singh M, et al. Success criteria in implant dentistry: A systematic review. *J Dent Res.* 2011;91: 242–248.
2. Albrektsson T, Sennerby L, Wennerberg A. State of the art of oral implants. *Periodontol 2000.* 2008;47:15–26.
3. Schroeder A, Van der Zypen E, Stich H, et al. The reaction of bone, connective tissue and epithelium to endosteal implants with titanium sprayed surfaces. *J Maxillofac Surg.* 1981;9:15–25.
4. Esposito M, Hirsch JM, Lekholm U, et al. Biological factors contributing to failures of osseointegrated oral implants (II): Etiopathogenesis. *Eur J Oral Sci.* 1998; 106:721–764.
5. Le Guéhennec L, Soueidan A, Layrolle P, et al. Surface treatments of titanium dental implants for rapid osseointegration. *Dent Mater.* 2007;23:844–854.
6. Carlsson L, Röstlund T, Albrektsson B, et al. Osseointegration of titanium implants. *Acta Orthop Scand.* 1986;57: 285–289.
7. Brånemark PI, Breine U, Adell R, et al. Intra-osseous anchorage of dental prostheses I: Experimental studies. *Scand J Plast Reconstr Surg.* 1969;3:81–100.
8. Brånemark PI, Hansson B, Adell R, et al. Osseointegrated implants in the treatment of edentulous jaw. Experience from a 10 year period. *Scand J Plast Reconstr Surg.* 1977;16:1–132.
9. Brånemark PI. Osseointegration and its experimental background. *J Prosthet Dent.* 1983;50:399–410.
10. Haberstroh KM. Hope for the short-term use of nanorough metallic implant formulations in the clinical arena. *Nanomedicine (Lond).* 2006;1:355–358.
11. Bucci-Sabattini V, Cassinelli C, Coelho PG, et al. Effect of titanium implant surface nanoroughness and calcium phosphate low impregnation on bone cell activity in vitro. *Oral Surg Oral Med Oral Pathol Oral Radiol Endod.* 2010;109:217–224.

12. Meirelles L. On Nano Size Structures for Enhanced Early Bone Formation. Department of Prosthodontics/Dental Material Science, Department of Biomaterials. Göteborg, Sweden: Göteborg University; 2007:70.
13. Wennerberg A, Albrektsson T. A review of current knowledge, opinions and suggestions for possible common mechanisms behind the increased bone response reported to different types of modern oral implant surfaces. *Int J Oral Maxillofac Implants*. 2010;25:63–74.
14. Deyneka-Dupriez N, Kocdemir B, Herr U, et al. Interfacial shear strength of titanium implants in bone is significantly improved by surface topographies with high pit density and microroughness. *J Biomed Mater Res B*. 2007;82B: 305–312.
15. Webster TJ, Eijofor JU. Increased osteoblast adhesion on nanophase metals: Ti, Ti6Al4V, and CoCrMo. *Biomaterials*. 2004;25:4731–4739.
16. Rebaudi A. The ray setting procedure: a new method for implant planning and immediate prosthesis delivery. *Int J Periodontics Restorative Dent*. 2007 Jun;27(3):267-75.
18. Buser D, Nydegger T, Oxland T, et al. Interface shear strength of titanium implants with a sandblasted and acid-etched surface: A biomechanical study in the maxilla of miniature pigs. *J Biomed Mater Res* 1999;45:75–83.
19. Buser D, Schenk RK, SS, Fiorellini JP, Fox CH, Stich H. Influence of surface characteristics on bone integration of titanium implants. A histomorphometric study in miniature pigs. *J Biomed Mater Res* 1991;25:889–902.
20. Abron A, Hopfensperger M, Thompson J, Cooper LF. Evaluation of a predictive model for implant surface topography effects on early osseointegration in the rat tibia model. *J Prosthet Dent* 2001;85:40–46.
21. Novaes ABJ, Souza SL, de Oliveira PT, Souza AM. Histomorphometric analysis of the bone-implant contact obtained with 4 different implant surface treatments placed side by side in the dog mandible. *Int J Oral Maxillofac Implants* 2002;17:377–383.
22. Wennerberg A, Albrektsson T. Suggested guidelines for the topographic evaluation of implant surfaces. *Int J Oral Maxillofac Implants* 2000;15:331–344.
23. Kilpadi D, Lemons J. Surface energy characterization of unalloyed titanium implants. *J Biomed Mater Res* 1994;28:1419–1425.
24. Vercaigne S, Wolke JGC, Naert I, Jansen JA. The effect of titanium plasma-sprayed implants on trabecular bone healing in the goat. *Biomaterials* 1998;19:1093–1099.
25. Stout KJ, Sullivan PJ, Dong WP, et al. The Development of Methods for the Characterization of Roughness in Three Dimensions. University of Birmingham and L'Ecole Centrale de Lyon. Elsevier, 1993.

26. Dong WP, Sullivan PJ, Stout KJ. Comprehensive study of parameters for characterizing 3-dimensional surface-topography. 2. Statistical properties of parameter variation. *Wear* 1993;167:9–21.
27. Dong WP, Sullivan PJ, Stout KJ. Comprehensive study of parameters for characterizing 3-dimensional surface-topography. 3. Parameters for characterizing amplitude and some functional-properties. *Wear* 1994;178:29–43.
28. Coelho PG, Granato R, Marin C, Teixeira HS. The effect of different implant macrogeometries and surface treatment in early biomechanical fixation: An experimental study in dogs. *J Mech Behav Biomed Mater* 2011;27:1974–1981.
29. Deporter D. Dental implant design and optimal treatment outcomes. *Int J Periodontics Restorative Dent* 2009;29:625–633.
30. Degidi M, Piattelli A. 7-year follow-up of 93 immediately loaded titanium dental implants. *J Oral Implantol* 2005;31:25–31.
31. Javed F, Romanos GE. The role of primary stability for successful immediate loading of dental implants. A literature review. *J Dent* 2010;38:612–620.
32. Elias CN, Rocha FA, Nascimento AL, Coelho PG. Influence of implant shape, surface morphology, surgical technique and bone quality on the primary stability of dental implants. *J Mech Behav Biomed Mater* 2012;16:169–180.
33. Cardoso MV, Vandamme K, Chaudhari A, et al. Dental implant macro-design features can impact the dynamics of osseointegration. *Clin Implant Dent Relat Res* 2015;17(4):639-45.
34. Naves MM, Menezes HHM, Magalhães D, Ferreira JA, Ribeiro SF, de Mello JDB, Costa, HL. Effect of macrogeometry on the surface topography of dental implants. *Int J Oral Maxillofac Implants*. 2015 Jul-Aug;30(4):789-99. doi: 10.11607/jomi.3934.
35. Goncalves JL Jr, Costa HL, Pessoa RS, de Mello JDB. 3D Topographic Characterization of Dental Implants. *Proceedings of The Third International Conference on Metrology*. 14-16 Nov, 2006. Annecy, 2012.
36. Rosa MB, Albrektsson T, Francischone CE, Filho HO, Wennerberg A. Micrometric characterization of the implant surfaces from the five largest companies in Brazil, the second largest worldwide implant market. *Int J Oral Maxillofac Implants* 2013;28:358–365.
37. Natali AN, Carniel EL, Pavan PG. Investigation of viscoelastoplastic response of bone tissue in oral implants press fit process. *J Biomed Mater Res B Appl Biomater* 2009a;2:868-875.
38. Natali AN, Carniel EL, Pavan PG. Dental implants press fit phenomena: biomechanical analysis considering bone inelastic response. *Dent Mater* 2009b;5:573-581.

39. Akca K, Chang TL, Tekdemir I, Fanuscu MI. Biomechanical aspects of initial intraosseous stability and implant design: a quantitative micro-morphometric analysis. *Clin Oral Implants Res* 2006;4:465-472.
40. Irinakis T, Wiebe C. Initial torque stability of a new bone condensing dental implant. A cohort study of 140 consecutively placed implants. *J Oral Implantol* 2009;6:277-282.
41. Rodrigo D, Aracil L, Martin C, Sanz M. Diagnosis of implant stability and its impact on implant survival: a prospective case series study. *Clin Oral Implants Res* 2010;21:255-261
42. Duyck J, Corpas L, Vermeiren S, Ogawa T, Quirynen M, Vandamme K, et al.. Histological, histomorphometrical, and radiological evaluation of an experimental implant design with a high insertion torque. *Clin Oral Implants Res* 2010;21:877-884.
43. Tabassum A, Meijer GJ, Wolke JG, Jansen JA. Influence of surgical technique and surface roughness on the primary stability of an implant in artificial bone with different cortical thickness: a laboratory study. *Clin Oral Implants Res* 2010;2:213-220.
44. Ricomini Filho AP, Fernandes FSF, Straioto FG, Silva WJ, Del Bel Cury AA. Preload loss and bacterial penetration on different implant-abutment connection systems. *Braz Dent J* 2010;21:123- 129.
45. Mints D, Elias C, Funkenbusch P, et al. Integrity of implant surface modifications after insertion. *Int J Oral Maxillofac Implants.* 2014;29:97–104.
46. Salerno M, Itri A, Frezzato M, Rebaudi A. Surface Microstructure of Dental Implants Before and After Insertion: An In Vitro Study by Means of Scanning Probe Microscopy. *Implant Dent* 2015;24:248–255.
47. Senna P, Del Bel Cury AA, Kates S, et al. Surface damage on dental implants with release of loose particles after insertion into bone. *Clin Implant Dent Relat Res* 2015;14(4);681-692
48. Misch CE. Implant design considerations for the posterior regions of the mouth. *Implant Dent.* 1999;8(4):376-86.
49. Ercoli C, Funkenbusch PD, Lee HJ, Moss ME, Graser GN The influence of drill wear on cutting efficiency and heat production during osteotomy preparation for dental implants: a study of drill durability. *Int J Oral Maxillofac Implants.* 2004 May-Jun;19(3):335-49.
50. Harris BH1, Kohles SS. Effects of mechanical and thermal fatigue on dental drill performance. *Int J Oral Maxillofac Implants.* 2001 Nov-Dec;16(6):819-26.
51. ISO/IS 11562. Metrological Characterization of Phase Correct Filters and Transmission Bands for Use in Contact (Stylus) Instruments. Geneva: International Organization for Standardization, 1993.

52. Albrektsson T, Wennerberg A. Oral implant surfaces: Part 1— Review focusing on topographic and chemical properties of different surfaces and in vivo responses to them. *Int J Prosthodont* 2004;17:536–543
53. Elias CN, Meirelles L. Improving osseointegration of dental implants. *Expert Rev Med Devices* 2010;7:241–256.
54. De Mello JDB, Durand-Charre M, Mathia T. Abrasion Mechanisms of white cast iron II: Influence of the metallurgical structure of V-Cr white cast irons. *Materials Science and Engineering*, 78 (1986) 127-134
55. Valverde GB, Jimbo R, Teixeira HS, Bonfante EA, Janal MN, Coelho PG. Evaluation of surface roughness as a function of multiple blasting processing variables. *Clin Oral Implants Res* 2013;24:238–242.

CAPÍTULO 3

IN VITRO ASSESSMENT OF THE LEVEL OF DEFORMATION IN EXTERNAL HEXAGON OF IMPLANT SUBJECTED TO INTERNAL TORQUE

Magalhães, Denildo; Naves, Marina Melo; Menezes, Helder Henrique Machado de; Bataglioni, César ; Magalhães, Guilherme Carminati; Santos-Filho, Paulo César. In vitro assessment of the level of deformation in external hexagon of implant subjected to internal torque. **Brazilian Dental Journal**, 2015.

External Hexagon Deformation in Implants Subjected to Internal Torque

Denildo Magalhães¹, Marina Melo Naves¹, Helder Henrique Machado Menezes², César Bataglion³, Guilherme Carminat Magalhães⁴, Paulo César Freitas Santos Filho⁵

Failures may occur in the connections of dental implants, especially in external hexagon (EH). Due to the deformations in this portion of implants, this study aimed to evaluate the levels of deformation of EH connections subjected to internal torque. Two types of implants were used: N group and S group. Torques of 0, 32, 45, 60 and 80 Ncm were applied to the N group, and torques of 0, 30, 40, 60 and infinite Ncm were applied to the S group implants. The internal distance (ID), internal area (IA) and external area (EA) of the EH were obtained from digital pictures, which were analyzed by a specific software. Statistical analysis was performed by the Scott-Knott test. The results showed that the higher the torque applied, the greater were the changes in the evaluated dimensions in both groups. In the S group, torque levels equal or greater than 40 Ncm and 30 Ncm caused greater deformation of EA and IA respectively, while in the N group, torque levels equal or greater than 60 Ncm and 32 Ncm caused greater deformation of EA and IA respectively. Levels of deformation were greater in the S group as compared with the N group. These findings suggest that the IA, EA and ID of the EH may be affected by different internal torque levels.

Introduction

In the last few years osseointegrated implants have provided important contributions to dental implant therapy and improvements in the functional and esthetic quality of edentulous rehabilitation. Considering that successful establishment and maintenance of osseointegration are affected by biomechanics (1), numerous studies have been conducted on the engineering properties of dental implants, e.g., the types of implant-abutment connections (2-4).

The external hexagon (EH) implant system was initially designed to transmit the rotational torque, which was applied on the external surface of the EH (external torque), for dental implant placement (5). Although these implants have been the most frequently performed, fatigue or overload failures such as deformation of the hexagon may occur during surgical placement of the implants, due to their different manufacturing tolerances. Higher insertion torque values reduce the risk of implant micromovements at the bone-implant interface, thereby obtaining higher rates of success of immediately loaded implants (6,7). On the other hand, implants can undergo morphological changes during torsion when inserted into bone (8). These changes, associated with the masticatory load, may affect the rotational freedom between implant and abutment and, hence, affect the implant/abutment stability (9-11).

Therefore, an accurate adaptation between the EH and the prosthetic component results in good biomechanical and aesthetic conditions for rehabilitation by osseointegrated implants (9).

Application of rotational force to the internal surface of the EH (internal torque) has been suggested to reduce the possibility of geometrical deformation of the EH (14), due to the greater resistance of the internal surface as compared to the external surface (9). These systems use the internal contact with the implant walls instead of mounting devices to apply the force, which simplifies the procedure and diminishes the cost of materials. However, system mechanisms will always reach limited resistance, and excessive torque may cause damage to the upper part of the implant, and to the connection to which prosthetic components are attached (13,14). In view of the possibility that external torque may affect the EH geometrical integrity, one may hypothesize that the application of internal forces may also cause changes in the EH external surface. The aim of this study was to evaluate, *in vitro*, the levels of deformation of EH following the application of internal torque.

Material and Methods

Forty implants (13.0 mm long x 3.75 mm wide, 4.1 mm platform) with EH and internal torque from two commercial

¹Department of Periodontology, Dental School, UFU - Federal University of Uberlândia, Uberlândia, MG, Brazil

²Department of Implantology, HD Post-graduation Dental School, Uberlândia, MG, Brazil

³Department of Prosthodontics, Ribeirão Preto Dental School, USP - São Paulo University, Ribeirão Preto, SP, Brazil

⁴Department of Post Graduation, Dental School, UFU - Federal University of Uberlândia, Uberlândia, MG, Brazil

⁵Department of Dental Materials, Dental School, UFU - Federal University of Uberlândia, Uberlândia, MG, Brazil

Correspondence: Prof. Dr. Denildo Magalhães, Avenida Pará, 1720 - Campus Umuarama - Bloco 4L - 38405-902 Uberlândia, MG, Brasil. Tel.: +55-34-3218-2255 / +55-34-99121-6665. e-mail: denildomagalhaes@gmail.com

Key Words: dental implants, abutment connection, torque.

brands - TitamaxTi implants (N group, 20 implants; Neodent, Curitiba, PR, Brazil) and Tryon implants (S group, 20 implants; SIN, São Paulo, SP, Brazil) were used (Figs. 1A and 1B). The implants were positioned in a stainless steel matrix (30 mm x 125 mm), with four regularly, linearly distributed 3.0 cm holes on the bottom and fixed in acrylic resin (VIPI Class, Pirassununga, SP, Brazil) in order to maintain a static positioning. These holes enabled stabilization of the implant in the matrix from outside using healing abutments (2 mm high), and also to simulate the final position of the implant in relation to the bone, i.e., the prosthetic fit at bone level and exposure of the implant.

Following the attachment of the implant to the stainless steel matrix, the matrix was lubricated with liquid paraffin (Farmax, Juiz de Fora, MG, Brazil), filled with chemically activated acrylic resin and heat-polymerized at 4.0 bar pressure for 10 min (Auto pressure polymerizer; Mestra Polyplus, Belo Horizonte, MG, Brazil). The models were then numbered from 1 to 4, and the implants identified with a number corresponding to the torque values, which were established based on the specifications given by the manufacturer of each group (N - Neodent / S - SIN), which were divided into 5 subgroups. In the N group, Model #1 (N0) did not receive torque and was used as control, Model #2 (N32) was subjected to a 32 Ncm torque, Model #3 (N45) to 45 Ncm torque, Model #4 (N60) to 60 Ncm torque and Model #5 (N80) to 80 Ncm torque. In the S group, Model #1 (S0) did not receive torque and was used as control, Model #2 (S30) was subjected to a 30 Ncm torque, Model #3 (S40) to 40 Ncm torque, Model #4 (S60) to 60 Ncm of torque and Model #5 (S∞) to infinite torque (>60 Ncm). Specific ratchet torque wrenches were used for each group, following the specifications set by the manufacturers (Figs. 2A and 2B), and one torque wrench was used for each implant model to avoid deformation of the wrench. The application of torques was performed by a single operator, who simulated the surgical procedure of dental implant, as follows: first the models were statically attached to a lathe, the operator positioned the internal wrench in the EH and then performed one slow, continuous, rotational movement,

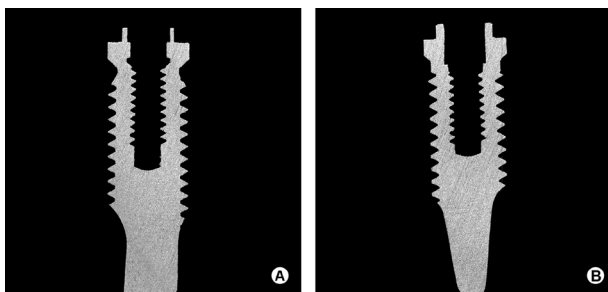


Figure 1. External and internal view of the N implant (A) and S implant (B).

until the desired torque was achieved. This procedure was repeated with all implant models (Figs. 3A and 3B).

The implants were photographed by a digital camera attached to a copy stand, which was positioned perpendicular to the hexagon and the platform before and after torque application. Hexagon deformation was calculated by the Image Tools 3.0 software (UTHSCSA, San Antonio, TX, USA), which was developed for image processing and analysis in terms of distance, angle, perimeter and area. Also, spatial calibration of the software enabled capturing the images in millimeters. The following EH measures were performed - internal dimensions (ID) (mm): distance between opposite vertices of the hexagon, measured on its internal face, with A2/B2/C2 defined as the distance between the two central points of opposite vertices, A1/B1/C1 defined as the distance between the points located at 0.25 mm to the left of each opposite vertex, A3/B3/C3 defined as the distance between the points located at 0.25 mm to the right of each opposite vertex; internal area (IA) (mm²) defined as the area of the EH internal face; and external area (EA) (mm²) defined as the area of the EH external face (Fig. 4). Mean values of ID, IA and EA obtained before and after torque application and the percentage of deformation were calculated. The Scott-Knott test was used for multiple comparisons, using a univariate cluster analysis (15).

Results

Means and standard deviations of ID deformation (%) by

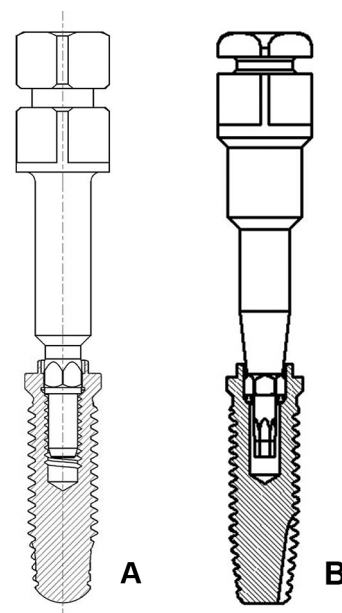


Figure 2. Implants of N group (A) and S group (B) and respective ratchet torque wrenches used for each group, following the specifications set by the manufacturers.

group are presented in Figures 5A and 5B. Increase in all EH measures was observed, which was related to the increase of torque. The measure with the greatest deformation percentage was A3/B3/C3.

The N60 and N80 implant models in the N group (Table 1) and the S60 and S∞ in the S group (Table 2) showed statistically significant ID deformation (%) for all measures. The IA and EA values are shown in Figures 6A and 6B. Similar initial and final mean values of IA and EA were obtained for N0 (IA: 3.70 mm²; EA: 6.40 mm²) and S0 (IA: 3.70 mm²; EA: 6.48 mm²). The other implants showed increased IA and EA values with the increase of torque, except for the EA of N32, N45 and S30 (Fig. 6A). In the N group, changes in the IA were equal or less than 0.09 mm² for N32, N45 and N60, and 0.13 mm² for N80. Changes in the EA were found in lesser extent than in IA, observed in N45 (0.01 mm²) and N60 (0.03 mm²) only. In the S group, except for the S30 model, significant increases in the IA and EA following torque application were observed for all implant models (Fig. 6B). The IA deformation values were 0.07 mm² (S30), 0.09 mm² (S45), 0.12 mm² (S60) and 0.14 mm² (S∞), and the EA deformation values were 0.03 mm² (S45), 0.11 mm² (S60) and 0.138 mm² (S∞).

D. Magalhães et al.

Discussion

The EH implant interface transmits the rotational force for insertion of the implant into the bone by applying an external or internal torque, whereas the EH/prosthetic abutment interface provides physical stability to the abutment on inserted implant. Both junctions require a dimensional freedom for an accurate, passive fit of the abutment to implant connection (4,11).

Deformations in the geometry of EH caused by external torque (16) have led to the use of internal torque, since the internal area of the implant exhibits greater resistance as compared to the external area. Therefore, in order to identify possible changes in the internal area of the implant

and to exclude interfering variables, the static positioning of the implants into the acrylic model was chosen for the application of torque in this study. This was highlighted by the comparisons between the implant models and the controls (N0 and S0), which showed similar initial and final measures and, hence, no EH deformation, as depicted in Figure 5 and Tables 1 and 2. Although the acrylic resin does not simulate bone tissue, it allowed excluding the effect of macrogeometry on susceptible movements of insertion torque.

Many factors may affect the quality of implant insertion, including bone density. When high values of torque are applied during EH implant surgical placement, the rotational freedom of the implant abutment can be increased due to changes in the internal angle or area of the EH. Any deformity on the external hexagon can derail prosthetic rehabilitation, especially in single crowns. The ID

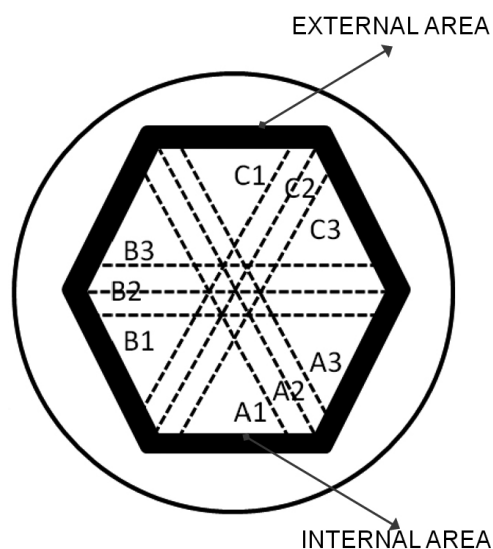


Figure 4. Representation of internal dimension measures, internal and external area of EH.



Figure 3. N group model (A) and S group model (B), used for torque application.

measures (Fig. 4) quantified the geometry of internal angles in relation to their equivalent opposites before and after the torque was applied. In both groups, the application of torques yielded changes in the evaluated measures (Tables 1 and 2). These changes were not statistically different in N32 and S30, indicating the capacity of these models to resist the torque applied by the operator. For N45 and S40 models, some measures (A2, B1, B3, C2 for N45 and A1, B1, B2, B3, C1, C3 for S40) showed significant deformation, suggesting that these models could also resist the torque applied, despite occurring some changes in the angle values. The other models (N60, N80, S60, S ∞) showed statistically significant changes for all measures, indicating an increased rotational freedom of the implant abutment. Figure 6 shows a progressive increase of all measures in both groups, illustrating a tendency for abutment displacement toward the rotational direction, i.e. the A3, B3 and C3 values were greater than the A2, B2 and C2 values, which were greater than the A1, B1 and C1 values, resulting in greater differences in the N group compared with the S group.

These changes could be identified by the determination of IA measurements, as it was observed increase in the internal area with the increase of the torque values (Fig. 6). It is noteworthy that the N60, N80, S40, S60 and S ∞ dimensions were near or greater than 0.1 mm², and thus capable to increase the rotational freedom of the implant. In addition, the standard deviation values were not high in

comparison with the means, indicating that the number of samples used in this study represents the behavior of EH in response to the torque applied. Therefore, considering that changes in both ID and IA occur simultaneously, it is important to consider the impact of such changes, especially in areas of higher bone density, on a greater rotational freedom of implant/abutment interface.

Passive fit between the screw-retained implant prosthesis and EH is fundamental for the biomechanical stability of the osseointegrated implant, which is negatively affected by changes on the external surface. In this study, although the application of torque caused changes in the ID and IA, most of the implant models showed minimal (N60) or no changes (N32, N45, S30) in the EA (Fig. 6). However, the level of changes observed in the EA of both N80 and S40, 0.59% (0.038 mm²) and 0.49% (0.032 mm²) respectively, may affect the correct fit of the prosthesis to the implant. Studies indicate a direct correlation between implant-abutment rotational misfit and screw loosening (10,16-19).

The greatest changes were observed in the S60 (1.69%, 0.110 mm²) and S ∞ models (2.12%, 0.138 mm²), exceeding the 0.1 mm² value, and hence hindering the EH/prosthetic abutment junction (7). The higher values of hexagon deformation for S group may be related to the morphology of the inner portion of the implant, where the connection key adapts. There is an internal stop for N implants that

Table 1. Results of multiple comparisons of internal dimension deformations (mm) at the measuring points (A1, A2, A3, B1, B2, B3, C1, C2 and C3) in response to different levels of torque in the N group

	A1	A2	A3	B1	B2	B3	C1	C2	C3
N0	0.000 ^a	0.000 ^a	0.000 ^a	0.000 ^a	0.000 ^a	0.000 ^a	0.000 ^a	0.000 ^a	0.000 ^a
N32	0.008 ^a	0.008 ^a	0.023 ^a	0.009 ^a	0.008 ^a	0.023 ^a	0.007 ^a	0.010 ^a	0.027 ^a
N45	0.010 ^a	0.018 ^b	0.034 ^a	0.014 ^b	0.019 ^a	0.035 ^b	0.012 ^a	0.019 ^b	0.033 ^a
N60	0.019 ^b	0.031 ^c	0.040 ^b	0.022 ^c	0.030 ^b	0.040 ^c	0.022 ^b	0.026 ^b	0.038 ^c
N80	0.024 ^b	0.040 ^d	0.045 ^b	0.027 ^c	0.036 ^b	0.044 ^d	0.027 ^b	0.036 ^c	0.044 ^c

Same letters between lines indicate lack of statistical difference; Scott-Knott test for multiple comparisons of the means; significance level of 0.05.

Table 2. Results of multiple comparisons of internal dimension deformations (mm) at the measuring points (A1, A2, A3, B1, B2, B3, C1, C2 and C3) in response to different levels of torque in the S group

	A1	A2	A3	B1	B2	B3	C1	C2	C3
s0	0.000 ^a	0.000 ^a	0.000 ^a	0.000 ^a	0.000 ^a	0.000 ^a	0.000 ^a	0.000 ^a	0.000 ^a
s30	0.009 ^a	0.012 ^a	0.032 ^a	0.012 ^a	0.012 ^a	0.030 ^a	0.011 ^a	0.015 ^a	0.032 ^a
s40	0.018 ^b	0.018 ^a	0.036 ^a	0.016 ^b	0.020 ^b	0.036 ^b	0.021 ^b	0.021 ^a	0.038 ^b
s60	0.023 ^b	0.031 ^b	0.042 ^b	0.031 ^c	0.029 ^c	0.041 ^b	0.018 ^c	0.031 ^b	0.042 ^c
s ∞	0.033 ^c	0.036 ^b	0.047 ^b	0.033 ^c	0.032 ^c	0.048 ^c	0.032 ^d	0.035 ^b	0.047 ^c

Same letters between lines indicate lack of statistical difference; Scott-Knott test for multiple comparisons of the means; significance level of 0.05.

may affect positively the resistance of hexagon, while the connection key of S implants is larger near external hexagon, touching this portion of S implants (Fig. 2). This fact may cause lower resistance on EH of S group. Although external hexagon implants using a mounting device present higher resistance to insertion torque compared with other systems with smaller hexagon connections or internal connections (20), it is important to analyze the geometry of internal connection according to the results of the present study.

These findings suggest that the IA, EA and ID of EH may be affected by different torque levels. These changes are directly related to the increase in torque and were greater in the S group compared with the N group. The importance of these comparative mechanical studies lies on the collection of information concerning the limitations of different EH connections, information of great clinical relevance. Since

were evaluated the levels of deformation of EH following the application of torque *in vitro*, it is suggested that the levels of deformation in dynamic conditions or clinical settings be investigated in further studies.

Resumo

Falhas podem ocorrer em conexões de implantes dentários, em especial em hexágonos externos (EH). Devido à ocorrência de deformação nesta porção dos implantes, este estudo objetivou avaliar os níveis de deformação de conexões EH submetidas ao torque interno. Dois tipos de implantes foram utilizados: grupo N e grupo S. Foram aplicados torques de 0, 32, 45, 60 e 80 Ncm nos implantes do grupo N e torques de 0, 30, 40, 60 Ncm e infinito nos implantes do grupo S. Medidas referentes à distância interna (ID), área interna (AI) e área externa (AE) foram obtidas por meio de fotos digitais analisadas em software. A análise estatística foi feita pelo teste de Scott-Knott. Os resultados demonstraram que quanto maior o torque aplicado, maior a alteração de todas as dimensões avaliadas em ambos os grupos. No grupo S, torques iguais ou superiores a 40 Ncm e 30 Ncm causaram maior deformação na AE e AI respectivamente, enquanto no grupo N, torques iguais ou superiores a 60 Ncm e 32 Ncm causaram

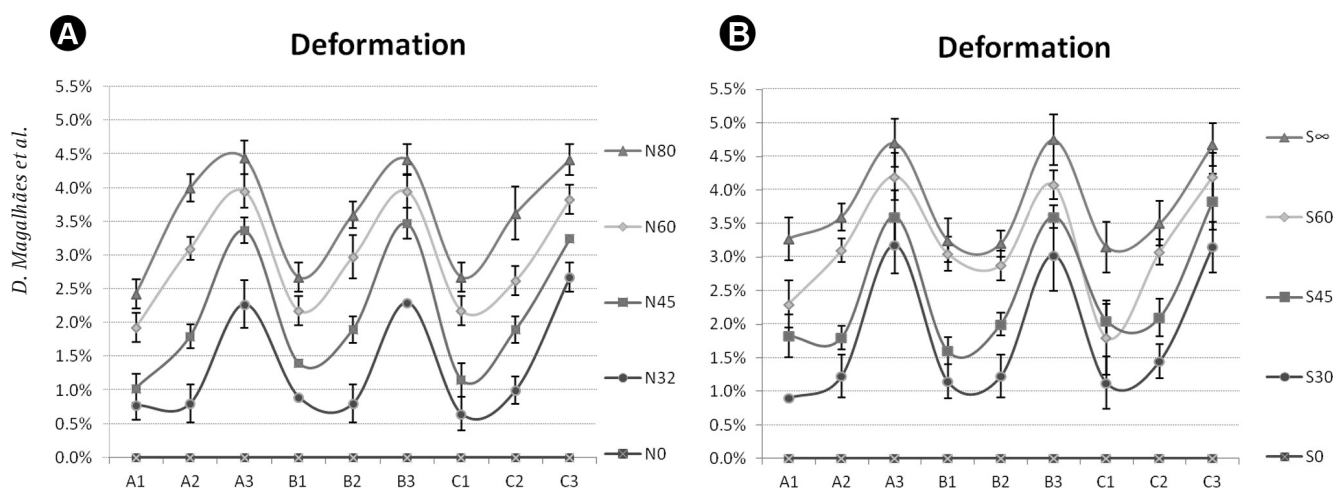


Figure 5. A: Mean and standard deviations of deformations (%) in response to the different levels of torque applied at points A1, A2, A3, B1, B2, B3, C1, C2 and C3 in the N group. B: Mean and standard deviations of deformations (%) in response to the different levels of torque applied at points A1, A2, A3, B1, B2, B3, C1, C2 and C3 in the S group.

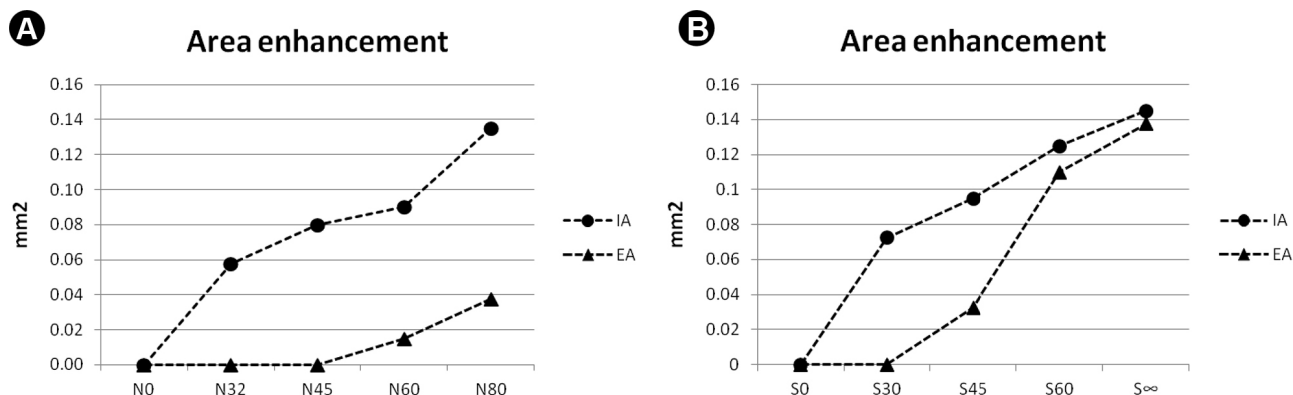


Figure 6. A: Internal and external areas (mm²) in response to the different levels of torque applied in the N group. B: Internal and external areas (mm²) in response to the different levels of torque applied in the S group.

maior deformação na AE e AI respectivamente. Os níveis de deformação foram maiores no grupo S em comparação ao grupo N. Nossos resultados indicam que a AI, a AE e a DI do EH podem ser influenciadas pelos diferentes torques internos.

Acknowledgements

The authors thanks to CNPq and FAPEMIG for the financial support, and Neodent® and SIN® for the research incentive.

References

1. Abuhussein H, Pagni G, Rebaudi A, Wang HL. The effect of thread pattern upon implant osseointegration. *Clin Oral Implants Res* 2010;21:129-136.
2. Almeida EO, Freitas Júnior AC, Bonfante EA, Rocha EP, Silva NR, Coelho PG. Effect of microthread presence and restoration design (screw versus cemented) in dental implant reliability and failure modes. *Clin Oral Implants Res* 2013;24:191-196.
3. Freitas Júnior AC, Bonfante EA, Silva NR, Marotta L, Coelho PG. Effect of implant-abutment connection design on reliability of crowns: regular vs. horizontal mismatched platform. *Clin Oral Implants Res* 2012;23:1123-1126.
4. Wicks RA, deRijk WG, Windeler AS. An evaluation of fit in osseointegrated implant components using torque/turn analysis. *J Prosthodont* 1994;3:206-212.
5. Branemark PI, Hansson BO, Adell R, Breine U, Lindström J, Hallén O, et al. Osseointegrated implants in the treatment of the edentulous jaw: experience from a 10-year period. *Scand J. Plast Reconstr Surg* 1977;16:1-132.
6. Trisi P, Perfetti G, Baldoni E, Berardi D, Colagiovanni M, Scogna G. Implant micromotion is related to peak insertion torque and bone density. *Clin Oral Implants Res* 2009;20:467-471.
7. Barbosa GAS, Simamoto Júnior PC, Fernandes Neto AJ, Mattos MGC, Neves FD. Prosthetic laboratory influence on the vertical misfit at the implant/UCLA abutment interface. *Braz Dent J* 2007;18:139-143.
8. Iijima M, Muguruma T, Brantley WA, Okayama M, Yuasa T, Mizoguchi I. Torsional properties and microstructures of miniscrew implants. *Am J Orthod Dentofacial Orthop* 2008;134:333.e1-6; discussion 333-334.
9. Binon PP, McHugh MJ. The effect of eliminating implant/abutment rotational misfit on screw joint stability. *Int J Prosthodont* 1996;9:511-519.
10. Vigolo P, Majzoub Z, Cordioli G. Measurement of the dimensions and abutment rotational freedom of gold-machined 3i UCLA-type abutments in the as-received condition, after casting with a noble metal alloy and porcelain firing. *J Prosthet Dent* 2000;84:548-553.
11. Vigolo P, Fonzi F, Majzoub Z, Cordioli G. An *in vitro* evaluation of ZiReal abutments with hexagonal connection: in original state and following abutment preparation. *Int J Oral Maxillofac Implants* 2005;20:108-14.
12. Merz BR, Hunenbart S, Belser UC. Mechanics of the implant- abutment connection: an 8-degree taper compared to a butt joint connection. *Int J Oral Maxillofac Implants* 2000;15:519-526.
13. Alsaadi G, Quirynen M, Michiels K, Jacobs R, van Steenberghe D. A biomechanical assessment of the relation between the oral implant stability at insertion and subjective bone quality assessment. *J Clin Periodontol* 2007;34:359-366.
14. Sakoh J, Wahlmann U, Stender E, Nat R, Al-Nawas B, Wagner W. Primary stability of a conical implant and a hybrid, cylindrical screw-type implant *in vitro*. *Int J Oral Maxillofac Implants*. 2006;21:560-566.
15. Scott AJ, Knott MA. A cluster analysis method for grouping means in the analysis of variance. *Biometrics*. Raleigh, v.30, n.3, 1974. p 507-512.
16. Davi LR, Golin AL, Bernardes SR, Araújo CA, Neves FD. *In vitro* integrity of implant external hexagon after application of surgical placement torque simulating implant locking. *Braz Oral Res* 2008;22:125-131.
17. Lang LA, Wang RF, May KB. The influence of abutment screw tightening on the screw joint configuration. *J Prosthet Dent* 2002;87:74-79.
18. Theoharidou A, Petridis HP, Tzannas K, Garefis P. Abutment screw loosening in single-implant restorations: a systematic review. *Int J Oral Maxillofac Implants* 2008;23:681-690.
19. Malaguti G, Denti L, Bassoli E, Franchi I, Bortolini S. Dimensional tolerances and assembly accuracy of dental implants and machined versus cast-on abutments. *Clin Implant Dent Relat Res* 2011;13:134-140.
20. Nary Filho H, Calvo Guirado JL, Matsumoto MA, Bresaola MD, Aur R. Biomechanical evaluation of resistance to insertion torque of different implant systems and insertion driver types. *Implant Dent* 2015 24:211-216.

Received September 13, 2014

Accepted May 22, 2015

3. CONSIDERAÇÕES GERAIS

- ✓ Os discos planos de titânio submetidos ao mesmo tratamento superficial não representam adequadamente a topografia de superfície de todas as regiões dos implantes, mas somente as regiões que tem angulação similar entre partículas abrasivas e superfícies;
- ✓ A macrogeometria dos implantes dentais tem forte influência nos parâmetros de rugosidade superficial dos implantes dentários. Logo, o conhecimento de um tipo de superfície aplicada a implantes dentários de macrogeometrias diferentes não é suficiente para caracterizar sua topografia final.
- ✓ A instalação de implantes dentários de diferentes macrogeometrias em osso pode alterar os parâmetros de rugosidade superficial, principalmente em implantes com maiores ângulos internos de rosca e área de topo maior. Parâmetros que caracterizam a distribuição de altura das irregularidades não são alterados significativamente.
- ✓ A geometria interna da conexão tipo hexágono externo tem forte influência na deformação deste tipo de conexão durante o processo de instalação de implantes dentários submetidos a torque interno. Quanto maior o torque aplicado, maior a deformação desta porção do implante.

REFERÊNCIAS

Abron A, Hopfensperger M, Thompson J, Cooper LF. Evaluation of a predictive model for implant surface topography effects on early osseointegration in the rat tibia model. **J Prosthet Dent**. 2001;85(1):40–6.

Alsaadi G, Quirynen M, Michiels K, Jacobs R, van Steenberghe D. A biomechanical assessment of the relation between the oral implant stability at insertion and subjective bone quality assessment. **J Clin Periodontol**. 2007;34(4):359–66.

Barikani H, Rashtak S, Akbari S, Fard MK, Rokn A. The effect of shape, length and diameter of implants on primary stability based on resonance frequency analysis. **Dent Res J (Isfahan)**. 2014;11(1):87–91.

Bennett JM, Mattsson L. Introduction to Surface Roughness and Scattering. 2nd Ed.; **Optical Society of America**. Washington, DC, 1999.

Branemark PI, Breine U, Adell R, Hansson B, Lindstrom J, Ohlsson A. Intraosseous anchorage of dental prostheses: I. Experimental studies. **Scand J Plast Reconstr Surg**. 1969;3(2):81–100.

Buser D, Nydegger T, Oxland T, Cochran DL, Schenk RK, Hirt HP, et al. Interface shear strength of titanium implants with a sandblasted and acid-etched surface: A biomechanical study in the maxilla of miniature pigs. **J Biomed Mater Res**. 1999;45(2):75–83.

Buser D, Schenk RK, SS, Fiorellini JP, Fox CH, Stich H. Influence of surface characteristics on bone integration of titanium implants. A histomorphometric study in miniature pigs. **J Biomed Mater Res**. 1991;25(7):889–902.

Cardoso VM, Vandamme K, Chaudhari A, De Rycker J, Van Meerbeek B, Naert I, Duyck J. Dental implant macro-design features can impact the dynamics of osseointegration. **Clin Implant Dent Relat Res**. 2015;17(4):639-45.

Chuang SK, Cai T. Predicting clustered dental implant survival using frailty methods. **J Dent Res**. 2015;17(4):639-45.

* De acordo com a Norma da FOUFU, baseado nas Normas de Vancouver. Abreviaturas dos periódicos com conformidade com Medline (Pubmed).

Coelho PG, Granato R, Marin C, Teixeira HS. The effect of different implant macrogeometries and surface treatment in early biomechanical fixation: An experimental study in dogs. **J Mech Behav Biomed Mater.** 2011;4(8):1974-81.

Degidi M, Piattelli A. 7-year follow-up of 93 immediately loaded titanium dental implants. **J Oral Implantol.** 2005;31(1):25-31.

Deporter D. Dental implant design and optimal treatment outcomes. **Int J Periodontics Restorative Dent.** 2009;29:625–633.

Dong SP, Mainsah E, Sullivan PJ, Stout KJ. Instruments and measurement techniques of 3-dimensional surface topography. In: Stout KJ (ed). *Three Dimensional Surface Topography: Measurement, Interpretation and Applications.* **London: Penton Press.** 1994a:3–63.

Dong WP, Sullivan PJ, Stout KJ. Comprehensive study of parameters for characterizing 3-dimensional surface-topography. 2. Statistical properties of parameter variation. **Wear.** 1993;167:9–21.

Dong WP, Sullivan PJ, Stout KJ. Comprehensive study of parameters for characterizing 3-dimensional surface-topography. 3. Parameters for characterizing amplitude and some functional-properties. **Wear** 1994b;178:29–43.

Duyck J, Roesems R, Cardoso MV, Ogawa T, De Villa Camargos G, Vandamme K. Effect of insertion torque on titanium implant osseointegration: an animal experimental study. **Clin Oral Implants Res.** 2015;26(2):191-6.

Elias CN, Rocha FA, Nascimento AL, Coelho PG. Influence of implant shape, surface morphology, surgical technique and bone quality on the primary stability of dental implants. **J Mech Behav Biomed Mater.** 2012;16:169-80

Fanuscu MI, Chang TL, Akca K. Effect of surgical techniques on primary implant stability and peri-implant bone. **J Oral Maxillofac Surg.** 2007;65(12):2487-91.

Goncalves JL Jr, Costa HL, Pessoa RS, de Mello JDB. 3D Topographic Characterization of Dental Implants. **Proceedings of The Third International Conference on Metrology,** (France) 21-23 March 2012.

Irinakis T, Wiebe C. Clinical evaluation of the NobelActive implant system: A case series of 107 consecutively placed implants and a review of the implant features. **J Oral Implantol.** 2009;35(6):283-8.

ISO 4287. Geometrical Product Specifications (GPS) – Surface Texture: Profile Method - Terms, Definitions and Surface Texture Parameters. Geneva: **International Organization for Standardization**, 1997.

Javed F, Romanos GE. The role of primary stability for successful immediate loading of dental implants. A literature review. **J Dent.** 2010;38(8):612-20.

Kilpadi D, Lemons J. Surface energy characterization of unalloyed titanium implants. **J Biomed Mater Res.** 1994;28(12):1419-25.

Levine RA, Clem D, Beagle J, Ganeles J, Johnson P, Solnit G. Multicenter retrospective analysis of the solid-screw ITI implant for posterior single-tooth replacements. **Int J Oral Maxillofac Implants** 2002;17(4):550–6.

Maeda Y, Satoh T, Sogo M. In vitro differences of stress concentrations for internal and external hex implant-abutment connections: A short communication. **J Oral Rehabil.** 2006;33(1):75-8

Naves MM, Menezes HH, Magalhães D, Ferreira JA, Ribeiro SF, de Mello JD, Costa HL. Effect of Macrogeometry on the Surface Topography of Dental Implants. **Int J Oral Maxillofac Implants.** 2015;30(4):789-99.

Neugebauer J, Scheer M, Mischkowski RA, An SH, Karapetian VE, Toutenburg H, Zoeller JE. Comparison of torque measurements and clinical handling of various surgical motors. **Int J Oral Maxillofac Implants.** 2009;24(3):469-76.

Novaes ABJ, Souza SL, de Oliveira PT, Souza AM. Histomorphometric analysis of the bone-implant contact obtained with 4 different implant surface treatments placed side by side in the dog mandible. **Int J Oral Maxillofac Implants.** 2002;17(3):377-83.

Rea M, Botticelli D, Ricci S, Soldini C, González GG, Lang NP. Influence of immediate loading on healing of implants installed with different insertion torques: An experimental study in dogs. **Clin Oral Implants Res.** 2015;26(1):90-5.

Rosa MB, Albrektsson T, Francischone CE, Filho HO, Wennerberg A. Micrometric characterization of the implant surfaces from the five largest

companies in Brazil, the second largest worldwide implant market. **Int J Oral Maxillofac Implants**. 2013;28(2):358-65

Rosa MB, Albrektsson T, Francischone CE, Schwartz Filho HO, Wennerberg A. The influence of surface treatment on the implant roughness pattern. **J Appl Oral Sci**. 2012;20(5):550-5.

Sakoh J, Wahlmann U, Stender E, Nat R, Al-Nawas B, Wagner W. Primary stability of a conical implant and a hybrid, cylindric screw-type implant in vitro. **Int J Oral Maxillofac Implants**. 2006;21(4):560-6.

Shibli JA, Grassi S, de Figueiredo LC, Feres M, Marcantonio E Jr, Iezzi G, Piattelli A. Influence of implant surface topography on early osseointegration: A histological study in human jaws. **J Biomed Mater Res B Appl Biomater**. 2007;80(2):377-85.

Shokri M, Daraeighadikolaei A. Measurement of primary and secondary stability of dental implants by resonance frequency analysis method in mandible. **Int J Dent**. 2013;2013:506968.

Soskolne WA, Cohen S, Sennerby L, Wennerberg A, Shapira L. The effect of titanium surface roughness on the adhesion of monocytes and their secretion of TNF-alpha and PGE2. **Clin Oral Implants Res**. 2002;13(1):86-93.

Stout KJ, Sullivan PJ, Dong WP, et al. The development of methods for the characterization of roughness in three dimensions. **University of Birmingham and L'Ecole Centrale de Lyon**, PUB no. EUR 15178EN, 1993.

Trisi P, Lazzara R, Rebaudi A, Rao W, Testori T, Porter SS. Bone implant contact on machined and dual acid-etched surfaces after 2 months of healing in the human maxilla. **J Periodontol**. 2003;74(7):945-56.

Trisi P, Perfetti G, Baldoni E, Berardi D, Colagiovanni M, Scogna G. Implant micromotion is related to peak insertion torque and bone density. **Clin Oral Implants Res**. 2009;20(5):467-71.

Vercaigne S, Wolke JGC, Naert I, Jansen JA. The effect of titanium plasma-sprayed implants on trabecular bone healing in the goat. **Biomaterials**. 1998;19(11-12):1093-9.

Wennerberg A, Albrektsson T. Suggested guidelines for the topographic evaluation of implant surfaces. **Int J Oral Maxillofac Implants**. 2000;15(3):331-44.

Zupnik J, Kim SW, Ravens D, Karimbux N, Guze K. Factors associated with dental implant survival: A 4-year retrospective analysis. **J Periodontol**. 2011;82(10):1390-5.